

# Re-thinking Spatial Confounding in Spatial Linear Mixed Models

Kori Khan<sup>1</sup> and Candace Berret<sup>2</sup>

<sup>1</sup>Department of Statistics, Iowa State University

<sup>2</sup>Department of Statistics, Brigham Young University

## Abstract

In the last two decades, considerable research has been devoted to a phenomenon known as spatial confounding. Spatial confounding is thought to occur when there is collinearity between a covariate and the random effect in a spatial regression model. This collinearity is considered highly problematic when the inferential goal is estimating regression coefficients, and various methodologies have been proposed to “alleviate” it. Recently, it has become apparent that many of these methodologies are flawed, yet the field continues to expand. In this paper, we offer the first attempt to synthesize work in the field of spatial confounding. We propose that there are at least two distinct phenomena currently conflated with the term spatial confounding. We refer to these as the analysis model and the data generation types of spatial confounding. We show that these two issues can lead to contradicting conclusions about whether spatial confounding exists and whether methods to alleviate it will improve inference. Our results also illustrate that in most cases, traditional spatial linear mixed models *do* help to improve inference of regression coefficients. Drawing on the insights gained, we offer a path forward for research in spatial confounding.

## 1 Introduction

In myriad applications, the use of standard regression models for spatially referenced data can result in spatial dependence in the residuals. For the better part of a century, the solution to this problem was to use a spatial regression model. In these models, a spatial random effect is introduced to account for

the residual spatial dependence and thereby (theoretically) improve inference, whether the inferential goal was associational or predictive.

This practice continued, unchallenged, until about two decades ago. At that time, a phenomenon now known as spatial confounding was introduced by Reich et al. (2006) and Hodges and Reich (2010) (see also, Paciorek, 2010). If, historically, spatial statisticians believed that incorporating spatial dependence with spatial regression models would improve inference; now those interested in spatial confounding suggest that incorporating spatial dependence with traditional models will distort inference. Originally focused on a setting where the estimation of individual covariate effects were important, interest in spatial confounding has since expanded to other inferential focuses (e.g., Page et al., 2017; Papadogeorgou et al., 2019). Spatial confounding is typically described as occurring when there is multicollinearity between a spatially-referenced covariate and a spatial random effect. It is thought to be quite problematic. For example, Marques et al. (2022) states spatial confounding can lead to “severely biased” regression coefficients, Reich et al. (2006) claims that it can lead to “large changes” in these estimates, and Prates et al. (2019) argues that both the “sign and relevance of covariates can change drastically” in the face of spatial confounding.

Despite the fact that many of these claims are not empirically supported, research into spatial confounding and methods to alleviate it has exploded (Hanks et al., 2015; Keller and Szpiro, 2020a; Adin et al., 2021; Marques et al., 2022; Hughes and Haran, 2013; Azevedo et al., 2021, 2022; Thaden and Kneib, 2018; Prates et al., 2019; Chiou et al., 2019; Dupont et al., 2022; Hefley et al., 2017; Hui and Bondell, 2021; Nobre et al., 2021). A closer look at the body of work highlights inconsistencies in definitions of spatial confounding as well as the purported impact it can have on inference (Khan and Calder, 2020; Zimmerman and Ver Hoef, 2021; Nobre et al., 2021; Hanks et al., 2015). Recently, many of the methods designed to alleviate spatial confounding have been shown to lead to counterintuitive results by Khan and Calder (2020) and have even been classified as “bad statistical practice” (Zimmerman and Ver Hoef, 2021). Yet, efforts to study and alleviate spatial confounding continue without any attempt to address these observations, increasingly influencing new fields of study such as causal inference and even criminology (Reich et al., 2021; Kelling et al., 2021)

In this paper, we (1) synthesize the existing body of work in spatial confounding, reviewing it in the context of historical teachings from spatial statistics; (2) characterize two distinct albeit related phenomena currently conflated with the term spatial confounding; and (3) show, through theoretical and simulation results, that these two issues can lead to contradicting

conclusions about whether spatial confounding exists and whether methods to alleviate it will actually improve inference. Importantly, by examining spatial confounding in this way, these three key understandings show how ignoring the nuances of “spatial confounding” can lead to methodologies that distort inferences in the very settings for which they are designed to be used.

The rest of this paper is organized as follows: In Section 2, we introduce the analytical set-up for the rest of the paper. Using this set-up, we provide an overview of spatial confounding in the broader context of spatial statistics. Section 3 provides a framework for understanding the two types of spatial confounding and illustrates how current (and past) research fits into this scheme. It also explores how efforts to mitigate spatial confounding can be organized into this framework. Section 4 introduces theoretical results assessing the impact of both sources of spatial confounding on bias for a regression coefficient. In Section 5, we use simulation studies to explore settings that have been identified in the literature as situations in which spatial confounding will lead to increased bias in regression coefficient settings. We illustrate that in these cases, traditional spatial analysis models often outperform both non-spatial models and models designed to alleviate spatial confounding. Finally, in Section 6, we propose a clear path towards resolving the contradictions explored in this paper.

## 2 Background

We begin by introducing the analytical set-up that will be used throughout the rest of the paper. We then use it to provide a brief history of how spatial confounding became a topic of concern in spatial statistics research and explore where it has gone since.

### 2.1 Analytical Set-Up

Throughout this paper, we distinguish between a *data generating* model and an *analysis* model. The former is a model meant to approximate how the data likely arose; while the latter is a model used to analyze the observed data.

Spatial regression models are traditionally used when there is residual spatial dependence after accounting for measured variables. Residual spatial dependence is thought to be the result of either an unobserved, spatially varying variable or an unobserved spatial process (Waller and Gotway, 2004). To define a data generating model, we focus on the former as this most closely matches the intuition motivating efforts to mitigate spatial confounding (see e.g., Reich

et al., 2006; Paciorek, 2010; Dupont et al., 2022; Page et al., 2017).

Specifically, we assume  $y_i$  is observed at location  $\mathbf{s}_i \in \mathbb{R}^2$  for  $i = 1, \dots, n$  and it can be modeled as follows:

$$\textbf{Generating Model: } y_i(\mathbf{s}_i) = \beta_0 + \beta_x x_i(\mathbf{s}_i) + \beta_z z_i(\mathbf{s}_i) + \epsilon_i, \quad (1)$$

where  $\mathbf{x}(\mathbf{s}) = (x_1(\mathbf{s}_1), \dots, x_n(\mathbf{s}_n))^T$  and  $\mathbf{z}(\mathbf{s}) = (z_1(\mathbf{s}_1), \dots, z_n(\mathbf{s}_n))^T$  are each univariate variables,  $\boldsymbol{\epsilon} = (\epsilon_1, \dots, \epsilon_n)^T$  is the vector of errors with mean  $\mathbf{0}$  and variance-covariance matrix  $\sigma^2 \mathbf{I}$ , and  $\boldsymbol{\phi} = (\beta_0, \beta_x, \beta_z, \sigma^2)^T$  are unknown.

Throughout this paper, we assume that  $\mathbf{x}(\mathbf{s})$  and  $\mathbf{y}(\mathbf{s})$  are observed and  $\mathbf{z}(\mathbf{s})$  is unobserved. We also assume that the primary inferential interest is on  $\beta_x$ . We consider three possible approaches to modeling the relationship between  $\mathbf{y}(\mathbf{s})$  and  $\mathbf{x}(\mathbf{s})$ : 1) A non-spatial linear approach, 2) a “traditional” spatial approach, and 3) an “adjusted” spatial approach. Each framework is associated with one or more analysis models that can be fit to the observed  $\mathbf{y}(\mathbf{s})$  and  $\mathbf{x}(\mathbf{s})$ .

$$\textbf{Non-Spatial Analysis Model: } y_i(\mathbf{s}_i) = \beta_0 + \beta_x^{NS} x_i(\mathbf{s}_i) + \epsilon_i \quad (2)$$

$$\textbf{Spatial Analysis Model: } y_i(\mathbf{s}_i) = \beta_0 + \beta_x^S x_i(\mathbf{s}_i) + g(\mathbf{s}_i) + \epsilon_i \quad (3)$$

$$\textbf{Adj. Spatial Analysis Model: } \tilde{y}_i(\mathbf{s}_i) = \beta_0 + \beta_x^{AS} \tilde{x}_i(\mathbf{s}_i) + h(\mathbf{s}_i) + \epsilon_i \quad (4)$$

For (2)–(4),  $\epsilon_i$  are i.i.d with mean 0 and unknown variance  $\sigma^2$ . The regression coefficients  $\beta_0$ ,  $\beta_x^{NS}$ ,  $\beta_x^S$ , and  $\beta_x^{AS}$  are unknown. We note that  $\sigma^2$  and  $\beta_0$  will vary based on the analysis model chosen. In other words, to be precise, we would use notation such as  $\beta_0^{NS}, \beta_0^S$ , and  $\beta_0^{AS}$ . As our primary interest is  $\beta_x$ , we refrain from doing so for the sake of simplicity.

The spatial random effects  $g(\mathbf{s})$  and  $h(\mathbf{s})$  are assumed to have mean zero and unknown, positive-definite variance-covariance matrices. We note that models relying on Gaussian Markov Random Fields (GMRFs) can be considered as special cases of this if the variance-covariance matrices are defined to be pseudo-inverses of the singular precisions (Paciorek, 2009). The tildes over  $\mathbf{y}(\mathbf{s})$  and  $\mathbf{x}(\mathbf{s})$  in (4) reflect that they may be functions of the originally observed  $\mathbf{y}(\mathbf{s})$  and  $\mathbf{x}(\mathbf{s})$  respectively. In future sections, we distinguish between a realization of the variables  $\mathbf{x}(\mathbf{s})$  and  $\mathbf{z}(\mathbf{s})$  and the stochastic processes that could have generated such realizations. We use capital letters (e.g.,  $\mathbf{X}(\mathbf{s})$  and  $\mathbf{Z}(\mathbf{s})$ ) to refer to stochastic processes and lower case letters to indicate a realization of the variables (e.g.,  $\mathbf{x}(\mathbf{s})$  and  $\mathbf{z}(\mathbf{s})$ ). After this, we drop notation indicating the dependence on spatial location unless it is needed for clarity.

## 2.2 Spatial Models

When there is residual spatial dependence, the conventional wisdom in spatial statistics literature is that a model which accounts for this spatial dependence will offer better inference than a model which does not account for it (Cressie, 1993; Bivand et al., 2008; Waller and Gotway, 2004). Historically, this view first appeared in the context of geostatistics and interpolation efforts. There, the goal was to improve predictions for the values of a stochastic process at unobserved locations (e.g., Wikle, 2010). In other words  $\beta_x^S$  in (3) was merely a tool to de-trend the data, and the primary interest was often estimating the variance-covariance matrix of the spatial random effect. The idea that accounting for spatial dependence improves inference later inspired many popular spatial models proposed for areal data. These models were often developed with the goal, either implicit or explicit, of ensuring that  $\beta_x^S$  in (3) was “close” to  $\beta_x$  in (1) (Besag et al., 1991; Hodges and Reich, 2010; Clayton et al., 1993). In recent decades, the lines delineating methods for geostatistical data and areal data have become blurred with advancements in computing and the popular class of models proposed by Diggle et al. (1998). However, across analysis goals and types of data, the consensus continued to be that models accounting for spatial dependence should be preferred over models that did not account for spatial dependence.

Recently, however, this view has shifted. The challenge to the prevailing view arose in a line of research about a phenomena now known as “spatial confounding”.

## 2.3 Spatial Confounding

Clayton et al. (1993) is often referenced as the first article to describe spatial confounding. These authors noticed what they referred to as “confounding by location”: estimates for regression coefficients changed when a spatial random effect was added to the analysis model. Clayton et al. (1993) interpreted this as a favorable change - one in which the estimates of the association between a response and an observed covariate was adjusted to account for an unobserved spatially-varying confounder (see also, Hodges and Reich, 2010). The modern conceptualization of spatial confounding arose in work by Reich et al. (2006) and Hodges and Reich (2010). These articles were the first to suggest that fitting spatial models could induce bias in the estimates of the regression coefficients and an “over-inflation” of the uncertainty associated with these estimates. These works have inspired a serious and active line of research into the phenomena

of spatial confounding (Hughes and Haran, 2013; Paciorek, 2010; Thaden and Kneib, 2018; Hefley et al., 2017; Nobre et al., 2021; Prates et al., 2019; Azevedo et al., 2021; Dupont et al., 2022; Yang et al., 2021; Marques et al., 2022).

Spatial confounding is almost always introduced as an issue of multicollinearity between a spatially varying covariate and a spatial random effect in a spatial analysis model (Reich et al., 2006; Hodges and Reich, 2010; Hefley et al., 2017; Reich et al., 2021; Dupont et al., 2022; Thaden and Kneib, 2018). This statement is often deemed sufficient to identify the phenomena of spatial confounding. However, there is no consensus on a formal definition for spatial confounding. While there have been two previous efforts to formalize spatial confounding, both were definitions considering special cases of a broader phenomena (Thaden and Kneib, 2018; Khan and Calder, 2020).

Despite the ambiguity of spatial confounding as a concept, researchers using the term have developed shared expectations for the phenomenon. These expectations have, in turn, shaped multiple methods aimed at alleviating spatial confounding. Some researchers have noticed inconsistencies and contradictions arising in some of the conclusions reached by the spatial confounding literature. For example, Hanks et al. (2015) and Nobre et al. (2021) have both observed that a distortion in inference for  $\beta_x$  can occur in the absence of stochastic dependence between  $\mathbf{x}$  and  $\mathbf{z}$ , contradicting some stated expectations for spatial confounding. These inconsistencies have largely remained unresolved even as research on spatial confounding has increasingly begun influencing other lines of work, such as causal inference (e.g., Reich et al., 2021; Papadogeorgou et al., 2019).

We propose that some of these contradictions arise because at least two distinct categories of issues are being studied by researchers in spatial confounding. Loosely speaking, we can think of these categories as encompassing a data generation phenomena and an analysis model phenomena. Importantly, once teased apart, these two issues can lead to different conclusions about whether spatial confounding is present and whether spatial analysis models should be adjusted.

### 3 Types of Spatial Confounding

As previously noted, spatial confounding is typically described as an issue of multicollinearity between a spatially varying covariate and a spatial random effect in a spatial analysis model. It appears, however, that researchers can disagree about the source of multicollinearity as well as what it means for a

covariate to be spatially varying (in a problematic sense). In this section, we tease apart what we refer to as data generation spatial confounding and analysis model spatial confounding. In Figure 1, we summarize how the problematic relationships that are thought to cause spatial confounding differ by type of spatial confounding, and we elaborate on these relationships shortly. We emphasize that this framework is not currently in use. Instead, it is a novel attempt meant to help organize some of the existing conceptualizations of spatial confounding in the literature. Importantly, many articles can have references to both types of spatial confounding within them. In the following discussion, we sort works based on the primary focus of the article.

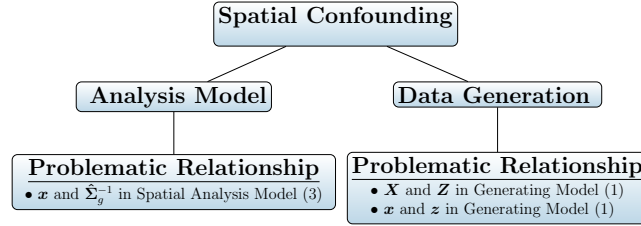


Figure 1: Primary Source of Spatial Confounding by Type

### 3.1 Analysis Model Spatial Confounding

Reich et al. (2006) and Hodges and Reich (2010) are the works that introduced the modern conceptualization of spatial confounding. These papers, and many of the works they inspired, focused on what we will refer to as analysis model spatial confounding. Research motivated by the analysis model issue often does not consider how  $\mathbf{y}$  or  $\mathbf{x}$  were generated. In other words, these works do not assume there is a missing  $\mathbf{z}$  or a data generation model of the form (1) (Hodges and Reich, 2010). Instead, this conceptualization of spatial confounding focuses on the relationship between an observed  $\mathbf{x}$  and the spatial random effect in a spatial analysis model (Reich et al., 2006; Hodges and Reich, 2010; Hughes and Haran, 2013; Hanks et al., 2015; Hefley et al., 2017; Prates et al., 2019; Azevedo et al., 2021; Hui and Bondell, 2021).

In this line of work, identifying the problematic source of multicollinearity and defining what it means for  $\mathbf{x}$  to be spatially varying both rely on the analysis model. More specifically, in the context of our analytical set-up, they typically rely on the eigenvectors of the estimated precision matrix  $\hat{\Sigma}_g^{-1}$  of the spatial random effect  $g(\mathbf{s})$  in (4) (Reich et al., 2006; Hanks et al., 2015; Hefley et al., 2017; Prates et al., 2019; Azevedo et al., 2021). For example, statistics developed

to identify spatial confounding involve using both the observed  $\mathbf{x}$  and the estimated precision matrix for a particular spatial analysis model (Reich et al., 2006; Hefley et al., 2017; Prates et al., 2019). These statistics all identify, loosely, whether  $\mathbf{x}$  is correlated with low-frequency eigenvectors of a decomposition of  $\hat{\Sigma}_g^{-1}$ . Similarly,  $\mathbf{x}$  is considered spatially varying (in a problematic sense) if it is highly correlated with such a low-frequency eigenvector of  $\hat{\Sigma}_g^{-1}$ . We note that, in spatial confounding literature, no one has precisely defined what it means for an eigenvector to be low-frequency (but see, Reich and Hodges, 2008). However, when displayed graphically, they tend to show spatial patterns where nearby things are more similar than others. Thus, the problematic relationship which causes data generation spatial confounding is thought to be primarily between  $\mathbf{x}$  and  $\hat{\Sigma}_g^{-1}$ , as summarized in Figure 1.

There are several common beliefs underlying work focused on this conceptualization of spatial confounding. First, spatial confounding occurs as a result of fitting a spatial analysis model. While a distortion to inference can be expected in any spatial analysis model (Hodges and Reich, 2010), it is plausible that the degree of distortion may vary based on the particular analysis model chosen (see e.g., Hefley et al., 2017). Second, efforts should be taken to determine whether spatial confounding needs to be adjusted for in the analysis model. In this line of work, many authors acknowledge that it not clear when spatial confounding needs to be accounted for (Prates et al., 2019; Hanks et al., 2015; Hui and Bondell, 2021). In other words, there is at least an implicit understanding that spatial analysis models may still be preferable over adjusted spatial analysis models at times. Finally, determining whether spatial confounding exists will involve studying characteristics of the observed data (in particular  $\mathbf{x}$ ) along with properties of the chosen analysis model.

### 3.2 Data Generation Spatial Confounding

In work that focuses on data generation spatial confounding, researchers often do assume that  $\mathbf{y}$  is generated from a model of the form (1). In the context of our analytical set-up, the interest is typically on how the relationship between  $\mathbf{X}$  or  $\mathbf{Z}$  (or alternatively  $\mathbf{x}$  and  $\mathbf{z}$ ) impacts inference on  $\beta_x^S$  when a spatial analysis model of the form (3) is used to fit the data (Paciorek, 2010; Thaden and Kneib, 2018; Page et al., 2017; Dupont et al., 2022; Nobre et al., 2021).

In this line of work, spatial confounding is still often defined as an issue of multicollinearity (Dupont et al., 2022; Thaden and Kneib, 2018). However, the source of the multicollinearity and the definition of spatially varying (in



the problematic sense) are not always clear. Paciorek (2010) has shaped much of the current work focused on data generation spatial confounding, as well as many of the most recent methods designed to alleviate spatial confounding (see e.g., Dupont et al., 2022; Thaden and Kneib, 2018; Page et al., 2017; Keller and Szpiro, 2020b; Marques et al., 2022). In that article and the many that followed, researchers make assumptions about the variables ( $\mathbf{x}$  and  $\mathbf{z}$ ) or the stochastic processes that generated them ( $\mathbf{X}$  and  $\mathbf{Z}$ ).

Researchers who focus on  $\mathbf{X}$  and  $\mathbf{Z}$  often assume that these processes are generated from spatial random fields parameterized by some set of known parameters (Paciorek, 2010; Page et al., 2017; Nobre et al., 2021).  $\mathbf{X}$  and  $\mathbf{Z}$  are typically assumed to be generated in such a way that  $\mathbf{X}$  has two components of spatial structure: 1) one that is shared with  $\mathbf{Z}$  (the confounded component), and 2) one that is not shared with  $\mathbf{Z}$  (the unconfounded component). Based on characteristics of these assumed processes, theoretical results or observations have been used to identify when fitting a spatial analysis model of the form (3) will distort inference on  $\beta_x$  (Paciorek, 2010; Nobre et al., 2021). In other words, the problematic relationship is between  $\mathbf{X}$  and  $\mathbf{Z}$ , as summarized in Figure 1.

Most of the theoretical results related to the data generation source of spatial confounding focus on  $\mathbf{X}$  and  $\mathbf{Z}$ . However, when it comes to methods designed to alleviate spatial confounding, there can be assumptions made about  $\mathbf{x}$  and  $\mathbf{z}$ . For example, Dupont et al. (2022) and Thaden and Kneib (2018) assume that  $\mathbf{x}$  is a linear combination of  $\mathbf{z}$  and Gaussian noise. In these cases,  $\mathbf{z}$  is either chosen to have a fixed spatial structure or is generated from a spatial random field or process. The focus on the relationship between  $\mathbf{X}$  and  $\mathbf{Z}$  suggests that the problematic multicollinearity is between  $\mathbf{x}$  and  $\mathbf{z}$ , as summarized in Figure 1. The fact that some methods designed to alleviate spatial confounding focus on situations where  $\mathbf{x}$  and  $\mathbf{z}$  are collinear lend support to this idea. However, the theoretical results in this line of work are usually not related to characteristics of the observed realization  $\mathbf{x}$  (or  $\mathbf{z}$ ), and the assumptions made in the theoretical results do not always ensure empirical collinearity between a given set of realizations  $\mathbf{x}$  and  $\mathbf{z}$ . In a similar manner, the characteristics of a particular realization  $\mathbf{x}$  are not assessed in determining whether it is spatially dependent in a problematic sense. It is possible that the underlying belief is that if  $\mathbf{x}$  and  $\mathbf{z}$  are collinear and “spatial”, then there will be collinearity between  $\mathbf{x}$  and a spatial random effect in an analysis model. However, papers in this line of work spend very little time discussing the impact of spatial analysis models. For example, Thaden and Kneib (2018) defines spatial confounding as occurring when: 1)  $\mathbf{X}$  and  $\mathbf{Z}$  are stochastically dependent, 2)  $E(\mathbf{Y}|\mathbf{X}, \mathbf{Z}) \neq E(\mathbf{Y}|\mathbf{X})$ , and

3)  $\mathbf{Z}$  has a “spatial” structure. Notice, that in this definition, the emphasis is on the relationship between  $\mathbf{X}$ ,  $\mathbf{Z}$ , and  $\mathbf{Y}$ , and it mirrors more general definitions of confounders in causal inference research. It is not entirely clear what it means for  $\mathbf{X}$  to have spatial structure or why it is problematic for  $\mathbf{X}$  to have such a structure. More importantly, by this definition, spatial confounding exists regardless of the analysis model chosen.

We note that not every paper completely ignores the analysis model. For example, Dupont et al. (2022) explicitly stated they were viewing spatial confounding from the perspective of fitting spatial models via thin plate splines. While they stated the smoothing that comes from fitting a spatial model contributes to the problem, the emphasis seemed to still be on the relationship between  $\mathbf{x}$  and  $\mathbf{z}$ . For example, the authors emphasized “if the correlation between the covariate and the spatial confounder is high, the smoothing applied to the spatial term in the model can disproportionately affect the estimate of the covariate effect.” In other words, it did not appear that the smoothing alone was problematic. It is for this reason we group this work here, rather than the analysis model spatial confounding, although we note this work is clearly one with elements of both types of spatial confounding.

We take a moment to highlight several notable beliefs commonly found in the data generation spatial confounding line of work. First, the primary source of spatial confounding comes from the (potentially unknown) process that generated the data rather than the process of fitting a model. Second, fitting a spatial analysis model will lead to distortion in inferences when spatial confounding is present. However, here, spatial analysis models – whether of the form of (3), a generalized additive model (GAM), or something else – are often treated as interchangeable. There is often no exploration of the impact of a particular choice of spatial model on inference, and inferior inferences for one type of spatial model are assumed to hold for other spatial models. Finally, it seems researchers assume the observed data (i.e.  $\mathbf{y}$  and  $\mathbf{x}$ ) do not give insight into whether spatial confounding is present or should be accounted for in analyses.

### 3.3 Approaches to Alleviating Spatial Confounding

There have been numerous methods designed to alleviate spatial confounding. In this sub-section, we take a moment to point out that most of them can be categorized as being motivated by either the analysis model or data generation type of spatial confounding.

The first methods to alleviate spatial confounding were motivated by the analysis model source of spatial confounding. For areal analyses, Reich et al. (2006) and Hodges and Reich (2010) first proposed a methodology sometimes known as restricted spatial regression. This method suggested to, in a sense, replace the spatial random effect  $g(\mathbf{s})$  in a spatial analysis model with a new spatial random effect  $h(\mathbf{s})$  in an adjusted spatial analysis model. This new spatial random effect is projected onto the orthogonal complement of the column space of  $\mathbf{x}$ . By “smoothing” orthogonally to the fixed effects, this methodology aimed to alleviate collinearity between the  $\mathbf{x}$  and the estimated variance-covariance matrix of  $h(\mathbf{s})$ . In doing so, it directly addresses the analysis model source of confounding. This approach motivated and continues to motivate many further methodologies designed to alleviate spatial confounding (Hughes and Haran, 2013; Hanks et al., 2015; Prates et al., 2019; Marques et al., 2022; Chiou et al., 2019; Hui and Bondell, 2021; Azevedo et al., 2021; Adin et al., 2021). Most of these methods continue to involve changing the spatial random effect (or analogue of it for other models) in the spatial analysis model. In other words, the adjustment from a model of the form (3) to (4) primarily involves replacing the spatial random effect and the data remains unaltered. As noted previously, these adjusted analysis models are typically offered with the caveat that there may be some situations when traditional analysis models would be more appropriate (although it is currently unclear when that is).

In this paper, we do not explore methods influenced by analysis model spatial confounding in the rest of the paper. Most of these methods have been influenced by restricted spatial regression analysis models. Recently, these models have been shown to perform poorly. Khan and Calder (2020) demonstrated that inference on  $\beta_x$  is often worse with restricted spatial regression analysis models than with non-spatial analysis models. Zimmerman and Ver Hoef (2021) subsequently offered a more in-depth, thorough review of restricted spatial regression analysis models. These authors showed that smoothing orthogonally to the fixed effects distorted inference for a variety of inferential goals and concluded that employing such analysis models was “bad statistical practice.”

Researchers motivated by data generation spatial confounding rely heavily on assumptions about how the data arose when developing methodology to alleviate spatial confounding. Thus, there can be various formulations. We focus on two methodologies proposed by Thaden and Kneib (2018) and Dupont et al. (2022) as illustrative examples of such approaches (described in more detail in Section 4.2). In both these works, the authors assume that the observed data are truly from a model with a form similar to (1) (in simulation studies Dupont

et al. (2022) introduced another unobserved spatial random effect to this model) and that  $\mathbf{x} = \beta_z \mathbf{z} + \boldsymbol{\epsilon}_x$ , where  $\boldsymbol{\epsilon}_x$  is Gaussian noise. Based on these assumptions, the authors proposed methodologies to alleviate spatial confounding that replace (or are equivalent to replacing) either  $\mathbf{y}$  or  $\mathbf{x}$  in the analysis model. The details of these approaches are given in Section 4.2.

Recall, Thaden and Kneib (2018) offered little discussion of the impact of the spatial analysis model on inference, and Dupont et al. (2022) felt that their proposed methodology would work in settings beyond the thin plate splines setting they explored. Subsequent work has claimed both approaches are useful for other types of spatial models (Schmidt, 2021; Dupont et al., 2022). As discussed in Section 3.2, this is characteristic of work motivated by data generation spatial confounding. The unspoken belief is that something must be known about how the data were generated to appropriately analyze it. If the data were truly generated in line with the assumptions made, the proposed methodologies should be superior to traditional spatial regression analysis models (and non-spatial analysis models).

In the rest of this paper, we give theoretical results that show that both the analysis model and data generation types of spatial confounding can impact inference, sometimes in competing ways. Importantly, we also show that methods designed to alleviate spatial confounding that focus on only one type of spatial confounding can, in some cases, distort inference more than a spatial regression model.

## 4 Two Views of Spatial Confounding Bias

In this section, we introduce theoretical results exploring the bias in estimates of  $\beta_x$  for various analysis models. We compare and contrast results derived with an emphasis on data generation and analysis model spatial confounding.

Throughout all sub-sections, we assume that data are originally generated from a model of the form (1). We consider a non-spatial analysis model of the form (2), spatial analysis models of the form (3), and adjusted spatial analysis models of the form (4). For the last category, we focus on the geoadditive structural equation modeling (GSEM) and Spatial+ approaches developed by Thaden and Kneib (2018) and Dupont et al. (2022) respectively (previously referenced in Section 3.3).

## 4.1 Bias: Non-Spatial and Spatial Analysis Models

In this sub-section, we consider how the data generation and analysis model types of spatial confounding may impact bias in the estimation of  $\beta_x$ . We consider this for the non-spatial analysis and spatial analysis models. To do so, we follow the set-up explored in Paciorek (2010). This article has shaped much of the current work focused on the data generation issue, as well as many of the most recent methods designed to alleviate spatial confounding (see e.g., Dupont et al., 2022; Thaden and Kneib, 2018; Page et al., 2017; Keller and Szpiro, 2020b; Marques et al., 2022).

Mirroring the work in Paciorek (2010), we begin by assuming that our response variable was generated from a model of the form Equation (1). However, instead of a particular set of realizations for  $\mathbf{x}$  and  $\mathbf{z}$ , we use the processes  $\mathbf{X}$  and  $\mathbf{Z}$ :

$$\mathbf{Y}(\mathbf{s}_i) = \beta_0 + \beta_x \mathbf{X}(\mathbf{s}) + \beta_z \mathbf{Z}(\mathbf{s}) + \epsilon_i, \quad (5)$$

where  $\epsilon_i$  is defined as in (1). We assume that  $\mathbf{X}$  and  $\mathbf{Z}$  are each generated from Gaussian random processes with positive-definite, symmetric covariance structures. In Paciorek (2010), the author considered two settings: one in which he stated there was no confounding in the data generation process and one in which he stated there was confounding in the data generation process. We restrict our attention to the situation where there is confounding in the data generation process.

Throughout this section, we assume  $\mathbf{X}$  and  $\mathbf{Z}$  are generated from Gaussian processes with Matérn spatial correlations:

$$\mathbf{C}(h|\theta, \nu) = \frac{1}{\Gamma(\nu)2^{\nu-1}} \left( \frac{2\sqrt{\nu}h}{\theta} \right)^\nu K_\nu \left( \frac{2\sqrt{\nu}h}{\theta} \right), \quad (6)$$

where  $h$  is the Euclidean distance between two locations,  $K_\nu$  is the modified Bessel function of the second order with smoothness parameter  $\nu$ , and  $\theta$  is the spatial range. We allow  $\mathbf{X} = \mathbf{X}_c + \mathbf{X}_u$ , where  $\text{Cov}(\mathbf{X}) = \sigma_c^2 \mathbf{C}(\theta_c) + \sigma_u^2 \mathbf{C}(\theta_u)$ ,  $\text{Cov}(\mathbf{Z}) = \sigma_z^2 \mathbf{C}(\theta_c)$ , and  $\text{Cov}(\mathbf{X}, \mathbf{Z}) = \rho \sigma_c \sigma_z \mathbf{C}(\theta_c)$ . We assume that  $\mathbf{C}(\theta_c)$  and  $\mathbf{C}(\theta_u)$  are each members of (6) with the same  $\nu$  and potentially different spatial range parameters. We stress that the source of confounding here is  $\rho$ , and the spatial aspect of the confounding is the shared spatial correlation functions in  $\mathbf{C}(\theta_c)$  and  $\mathbf{C}(\theta_u)$ . There is no guarantee that a particular set of realizations  $\mathbf{x}$  and  $\mathbf{z}$  will be collinear or share specific spatial patterns.

#### 4.1.1 Data Generation Confounding

We first explore bias from the perspective of data generation spatial confounding. Work on data generation confounding tends to treat  $\mathbf{X}$  and  $\mathbf{Z}$  stochastically when deriving bias terms (Paciorek, 2010; Page et al., 2017). When considering bias for a spatial regression analysis model, generalized least squares estimators are used. We adopt this approach here.

In Remark 1 we calculate the bias terms  $\text{Bias}(\beta_x^{NS}|\mathbf{X}^*) = \beta_x - E(\hat{\beta}^{NS}|\mathbf{X}^*)$ , for a non-spatial regression analysis model, and  $\text{Bias}(\beta_x^S|\mathbf{X}^*) = \beta_x - E(\hat{\beta}^S|\mathbf{X}^*)$ , for a spatial regression analysis model of the form (3). Here,  $\mathbf{X}^* = [\mathbf{1} \ \mathbf{X}]$ .

**Remark 1.** Let the data generating model be of the form (5) with  $\mathbf{X} = \mathbf{X}_c + \mathbf{X}_u$  and  $\mathbf{Z}$  having the following characteristics:

1.  $\text{Cov}(\mathbf{X}) = \sigma_c^2 \mathbf{C}(\theta_c) + \sigma_u^2 \mathbf{C}(\theta_u)$
2.  $\text{Cov}(\mathbf{Z}) = \sigma_z^2 \mathbf{C}(\theta_c)$ , and
3.  $\text{Cov}(\mathbf{X}, \mathbf{Z}) = \rho \sigma_c \sigma_z \mathbf{C}(\theta_c)$

where  $\mathbf{C}(\theta_c)$  and  $\mathbf{C}(\theta_u)$  are of the form (6) with the same  $\nu$ . If a non-spatial analysis model of the form (2) is employed with variance parameters assumed known, then the  $\text{Bias}(\beta_x^{NS}|\mathbf{X}^*) = \beta_x - E(\hat{\beta}_X^{NS}|\mathbf{X}^*)$  can be expressed as:

$$\beta_z \rho \frac{\sigma_z}{\sigma_c} \left[ \left( \mathbf{X}^{*T} \mathbf{X}^* \right)^{-1} \mathbf{X}^{*T} \mathbf{K} (\mathbf{X} - \mu_x \mathbf{1}) \right]_2 \quad (7)$$

If instead, a spatial analysis model of the form (3) is employed with variance parameters assumed known, then  $\text{Bias}(\beta_x^S|\mathbf{X}^*) = \beta_x - E(\hat{\beta}_X^S|\mathbf{X}^*)$  can be expressed as:

$$\beta_z \rho \frac{\sigma_z}{\sigma_c} \left[ \left( \mathbf{X}^{*T} \boldsymbol{\Sigma}^{-1} \mathbf{X}^* \right)^{-1} \mathbf{X}^{*T} \boldsymbol{\Sigma}^{-1} \mathbf{K} (\mathbf{X} - \mu_x \mathbf{1}) \right]_2 \quad (8)$$

where  $\mathbf{K} = p_c \left( p_c \mathbf{I} + (1 - p_c) \mathbf{C}(\theta_u) \mathbf{C}(\theta_c)^{-1} \right)^{-1}$ ,  $p_c = \frac{\sigma_c^2}{\sigma_c^2 + \sigma_u^2}$ ,  $\boldsymbol{\Sigma} = \beta_z^2 \sigma_z^2 \mathbf{C}(\theta_c) + \sigma^2 \mathbf{I}$ , and  $[\ ]_2$  indicates the second element of the vector.

*Proof.* See Appendix B.1 and Appendix B.2 for derivations.  $\square$

We note that (8) is equivalent to Equation (6) in Paciorek (2010) when  $\nu = 2$ . The bias terms (7) and (8) are very complicated. We take a moment to point out several things. First, for the spatial model the “true” precision

of  $\mathbf{Y}$  (conditional on  $\mathbf{X}$ ),  $\Sigma^{-1}$ , is used, effectively ignoring the impact of the particular analysis model chosen. As we have discussed, this is very common in explorations of bias influenced by the data generation spatial confounding. However, we note that Paciorek (2010) did include a brief description of the impact of analysis models in Section 2.1 of that paper. Second, it is difficult to derive insights from these forms of bias. They are heavily dependent not only on the spatial range parameters and the various other variance parameters, but also on the distributional assumptions on  $\mathbf{X}$ .

In Paciorek (2010), he measured the bias due to spatial confounding with the term  $c_S(\mathbf{X}) = \left(\mathbf{X}^{*T}\Sigma^{-1}\mathbf{X}^*\right)^{-1}\mathbf{X}^{*T}\Sigma^{-1}\mathbf{K}(\mathbf{X} - \mu_x\mathbf{1})$  from Remark 1. Here, we also introduce the non-spatial equivalent  $c_{NS}(\mathbf{X}) = \left(\mathbf{X}^{*T}\mathbf{X}^*\right)^{-1}\mathbf{X}^{*T}\mathbf{K}(\mathbf{X} - \mu_x\mathbf{1})$  from Remark 1. More specifically, he considered  $E_{\mathbf{X}}(c_S(\mathbf{X}))$ . To control for the influence for the marginal variance parameters and  $\beta_z$ , he calculated (via simulations)  $E_{\mathbf{X}}(c_S(\mathbf{X}))$  for various values of  $p_c$  (defined in Remark 1) and the term  $p_z = \frac{\beta_z^2\sigma_z^2}{\beta_z^2\sigma_z^2 + \sigma^2}$ . He did this for the case where  $\mathbf{C}(\theta_c)$  and  $\mathbf{C}(\theta_u)$  are members of (6) with  $\nu = 2$ .

The results, replicated from his code available at <https://www.stat.berkeley.edu/~paciorek/research/code/code.html>, suggested that a spatial regression analysis model could result in reduced bias relative to a non-spatial analysis when  $\theta_u \ll \theta_c$ . On the other hand, a spatial regression analysis could also increase bias relative to a non-spatial analysis when  $\theta_u \gg \theta_c$ . To see this, note that Paciorek (2010) stated that  $E_{\mathbf{X}}(c_{NS}(\mathbf{X})) \approx p_c$ . It can also be shown that  $E_{\mathbf{X}}(c_S(\mathbf{X})) \approx p_c$  when  $\theta_c = \theta_u$ . Figure 2 provides images of  $E_{\mathbf{X}}(c_S(\mathbf{X}))$  for 100 locations on a grid of the unit square for different fixed values of  $p_c$ ,  $p_v$ ,  $\theta_c$ , and  $\theta_u$  when  $\nu = 2$ . The upper left subplot of the image matrix provides a colored image of  $E_{\mathbf{X}}(c_S(\mathbf{X}))$  when  $p_c = p_z = 0.1$  and  $\theta_c$  varies from 0 to 1 (x-axis) and  $\theta_u$  varies from 0 to 1 (y-axis). As  $\theta_c$  increases, holding all else constant,  $E_{\mathbf{X}}(c_S(\mathbf{X}))$  decreases. In contrast, as  $\theta_u$  increases, holding all else constant,  $E_{\mathbf{X}}(c_S(\mathbf{X}))$  increases. Moving to the other subplots within the image matrix shows the same colored representation of  $E_{\mathbf{X}}(c_S(\mathbf{X}))$ , but for different values of  $p_c$  and  $p_z$ . As either  $p_c$  or  $p_z$  increase,  $E_{\mathbf{X}}(c_S(\mathbf{X}))$  also increases. Notice, however, that for any given value of  $p_c$  and  $p_z$ , we see the same behavior for  $E_{\mathbf{X}}(c_S(\mathbf{X}))$  as  $\theta_u$  and  $\theta_c$  changes that we saw in the first subplot considered. Namely that reduced bias is observed when  $\theta_u \ll \theta_c$ .

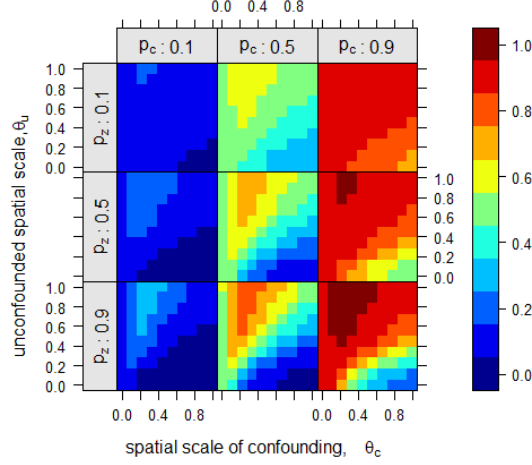


Figure 2: This image depicts  $E_{\mathbf{X}}(c_S(\mathbf{X}))$  for 100 locations on a grid of the unit square when  $\mathbf{C}(\theta_u)$  and  $\mathbf{C}(\theta_c)$  belong to the Matérn class with  $\nu = 2$ . Recall,  $E_{\mathbf{X}}(c_{NS}(\mathbf{X})) \approx p_c$ , and  $E_{\mathbf{X}}(c_S(\mathbf{X})) \approx p_c$  when  $\theta_c = \theta_u$ . Thus, terms lower than the diagonal represent a reduction in bias by modeling the residual spatial dependence. This image was created from Christopher Paciorek’s code using the `fields` and `lattice` packages (Sarkar, 2008; Douglas Nychka et al., 2021).

Paciorek (2010) explicitly acknowledged that the case where  $\theta_u \gg \theta_c$  is likely of limited interest in real applications. However, this case has increasingly influenced further research in spatial confounding. Or rather, the fact that bias for a spatial analysis model can be increased relative to the bias for a non-spatial model has influenced further research. Other papers often use this observation to support statements suggesting that spatial confounding occurs when “spatial range of the observed risk factors is larger than the unobserved counterpart” (Marques et al., 2022). However, it is rarely acknowledged that these simulations considered only a very specific case (there are exceptions, see e.g., Keller and Szpiro, 2020b).

In the context of data generation spatial confounding, this can be problematic because the behavior of bias from spatial confounding is so dependent on the distributional assumptions for  $\mathbf{X}$ . To illustrate this issue, we now repeat the simulation study for the case when  $\mathbf{C}(\theta_c)$  and  $\mathbf{C}(\theta_u)$  are members of (6) with  $\nu = .5$ . Here, the spatial process is less smooth than the case considered in Paciorek (2010). As in Paciorek (2009), for this case  $E_{\mathbf{X}}(c_{NS}(\mathbf{X})) \approx p_c$ , and  $E_{\mathbf{X}}(c_S(\mathbf{X})) \approx p_c$  when  $\theta_c = \theta_u$ . For small values of



$\theta_u$  and  $\theta_c$ , it turns out that the images can look fairly flat. To better illustrate trends, we consider values of  $\theta_u$  and  $\theta_c$  up to 10. In Figure 3, we see the bias modification term is almost always equal to the non-spatial equivalent. It appears that bias reduction can occur when  $\theta_u$  is less than 2, regardless of the value of  $\theta_c$ . Similarly, bias can be increased when  $\theta_c$  is less than 2, across all values of  $\theta_u$ . In other words, there is no longer strong evidence to support statements that spatial confounding impacts bias when the “spatial range of the observed risk factors is larger than the unobserved counterpart.”

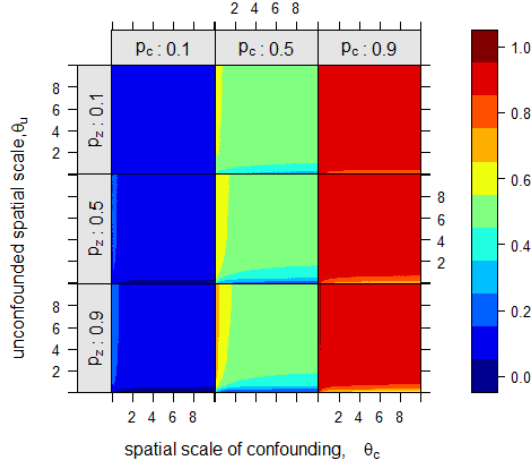


Figure 3: This image depicts  $E_{\mathbf{X}}(c_S(\mathbf{X}))$  for locations on grid of the unit square when  $\mathbf{C}(\theta_u)$  and  $\mathbf{C}(\theta_c)$  belong to the Matérn class  $\nu = .5$ . Again,  $E_{\mathbf{X}}(c_{NS}(\mathbf{X})) \approx p_c$ , and  $E_{\mathbf{X}}(c_S(\mathbf{X})) \approx p_c$  when  $\theta_c = \theta_u$ . Thus, terms lower than the diagonal represent a reduction in bias by modeling the residual spatial dependence. This images was created from an adaptation of Christopher Paciorek’s code using the `fields` and `lattice` packages (Sarkar, 2008; Douglas Nychka et al., 2021).

Importantly, these examples illustrate how sensitive our conclusions about the impact of spatial confounding are to the distributional assumptions we make about  $\mathbf{X}$  and  $\mathbf{Z}$ .

#### 4.1.2 Analysis Model Source of Spatial Confounding

In this sub-section, we focus on the analysis model type of spatial confounding. In order to make our results comparable to the setting explore in Section 4.1.1,

we assume that for a particular set of realizations  $\mathbf{x}$  and  $\mathbf{z}$ , the response  $\mathbf{y}$  is generated from a model of the form Equation (1). We can assume that the processes  $\mathbf{X}$  and  $\mathbf{Z}$  are generated as before. However, the results in this section do not depend on any distributional assumptions about  $\mathbf{X}$  and  $\mathbf{Z}$ . Unlike in Section 4.1.1, we assume that all variance parameters are unknown. As we will see, this results in conceptualizing spatial confounding by the relationships that the  $\mathbf{x}$ ,  $\mathbf{y}$ , and  $\mathbf{z}$  have with the eigenvectors of an estimated precision matrix  $\hat{\Sigma}^{-1}$ .

We consider both the non-spatial analysis model and the class of spatial analysis models of the form (3). First, in Lemma 1, we derive the bias term that results from fitting a non-spatial analysis model.

**Lemma 1.** *Let the data generating model be of the form (1) with  $\mathbf{y}$  and  $\mathbf{x}$  known. If a non-spatial analysis model of the form (2) is fit, then  $\text{Bias}(\hat{\beta}_x^{NS}) = \beta_x - E(\hat{\beta}_x^{NS})$  can be expressed as:*

$$\frac{\beta_z}{\|\mathbf{1}\|^2 \|\mathbf{x}\|^2 - [\langle \mathbf{x}, \mathbf{1} \rangle]^2} (\|\mathbf{1}\|^2 \langle \mathbf{x}, \mathbf{z} \rangle - \langle \mathbf{x}, \mathbf{1} \rangle \langle \mathbf{z}, \mathbf{1} \rangle),$$

where  $\langle \cdot, \cdot \rangle$  is the standard Euclidean inner product and  $\|\cdot\|$  represents the norm induced by it.

Because this ends up being a special case of the bias for the GLS estimators discussed next, we delay a discussion of these terms. Now, we assume that we fit a spatial analysis model of the form (3).

**Lemma 2.** *Let the data generating model be of the form Equation (1) with  $\mathbf{y}$  and  $\mathbf{x}$  known. If a spatial analysis model of the form (3) is fit, and results in the positive definite estimate  $\hat{\Sigma}$ , then the bias  $\text{Bias}(\hat{\beta}_x^S) = \beta_x - E(\hat{\beta}_x^S)$  can be expressed as:*

$$\frac{\beta_z}{\|\mathbf{1}\|_{\hat{\Sigma}^{-1}}^2 \|\mathbf{x}\|_{\hat{\Sigma}^{-1}}^2 - [\langle \mathbf{x}, \mathbf{1} \rangle_{\hat{\Sigma}^{-1}}]^2} (\|\mathbf{1}\|_{\hat{\Sigma}^{-1}}^2 \langle \mathbf{x}, \mathbf{z} \rangle_{\hat{\Sigma}^{-1}} - \langle \mathbf{x}, \mathbf{1} \rangle_{\hat{\Sigma}^{-1}} \langle \mathbf{z}, \mathbf{1} \rangle_{\hat{\Sigma}^{-1}}). \quad (9)$$

*Proof.* See Appendix B.4 for the calculations.  $\square$

Here, the estimate of precision matrix  $\Sigma^{-1}$  is  $\hat{\Sigma}^{-1}$ . We define the inner product  $\langle m, n \rangle_{\hat{\Sigma}^{-1}} = m^T \hat{\Sigma}^{-1} n$  for  $m, n \in \mathbb{R}^n$ , and we let  $\|\cdot\|_{\hat{\Sigma}^{-1}}$  be the norm induced by it (see Appendix A for more details). We do not make any assumptions of how the term  $\hat{\Sigma}^{-1}$  is estimated (e.g., Bayesian vs. residual maximum likelihood), but we acknowledge two different methods of fitting the same analysis model could result in different  $\hat{\Sigma}^{-1}$ . Finally, we note in Remark 2 that the bias term in Lemma 1 is a special case of the bias term in Lemma 2.

**Remark 2.** When  $\hat{\Sigma}^{-1} = \mathbf{I}$ ,  $\text{Bias}\left(\hat{\beta}_x^{NS}\right)$  in Lemma 1 is a special case of  $\text{Bias}\left(\hat{\beta}_x^S\right)$  in Lemma 2.

The bias term in (9) is a function of  $\beta_z$ , which makes intuitive sense. Although this will, of course, not be known, we note that its impact on inference is the same across all analysis models belonging to the spatial analysis models as well as the non-spatial analysis model. For the moment, we focus on the other terms. We begin with the numerator of (9) (ignoring  $\beta_z$ ):

$$\|\mathbf{1}\|_{\hat{\Sigma}^{-1}}^2 \langle \mathbf{x}, \mathbf{z} \rangle_{\hat{\Sigma}^{-1}} - \langle \mathbf{x}, \mathbf{1} \rangle_{\hat{\Sigma}^{-1}} \langle \mathbf{z}, \mathbf{1} \rangle_{\hat{\Sigma}^{-1}}. \quad (10)$$

Broadly speaking, this term tends to get smaller when one of two things happens. The first situation occurs when the low frequency eigenvectors of  $\hat{\Sigma}^{-1}$  are “flat”. We say an eigenvector is “flat” if it there is a small angle (with respect to the Euclidean norm) between it and the column vector of ones,  $\mathbf{1}$ . We say an eigenvector is “low-frequency” if its associated eigenvalue is less than 1. When this occurs, all terms involving  $\mathbf{1}$  (i.e.,  $\|\mathbf{1}\|_{\hat{\Sigma}^{-1}}^2$ ,  $\langle \mathbf{x}, \mathbf{1} \rangle_{\hat{\Sigma}^{-1}}$ , and  $\langle \mathbf{z}, \mathbf{1} \rangle_{\hat{\Sigma}^{-1}}$ ) will become smaller in magnitude. To illustrate this, we randomly generate locations for 140 observations on a  $[0, 10] \times [0, 10]$  window. Using these locations, we represent different potential  $\hat{\Sigma}^{-1}$ ’s by calculating the inverses of variance-covariance matrices for members of the Matérn class. In Figure 4, we use colors to denote three possible values of  $\nu$ :  $\nu = .5$  (the exponential),  $\nu = 1$  (Whittle), and  $\nu = 2$ . For fixed  $\nu$ , we then calculate various variance-covariance matrices by allowing  $\theta$  to vary. For the inverse of each unique matrix, we calculate  $\|\mathbf{1}\|_{\hat{\Sigma}^{-1}}$ . For fixed  $\nu$ , we can expect the lowest frequency eigenvectors of the eigendecomposition of the associated  $\hat{\Sigma}^{-1}$  to become flatter as  $\theta$  increases. In Figure 4(a), we can see that  $\|\mathbf{1}\|_{\hat{\Sigma}^{-1}}$  decreases in magnitude as  $\theta$  increases for all values of  $\nu$ . This trend will also be seen in cross-products involving  $\mathbf{1}$ , as can be seen in Figure 4b). Note that in these plots, the black line denotes the Euclidean norm. Almost all of the values of  $\|\mathbf{1}\|_{\hat{\Sigma}^{-1}}$  are less than this in magnitude. In many practical situations where spatial covariance matrices are employed, this will tend to happen.

The second situation that will tend to decrease the magnitude of (10) occurs when there are small angles (again with respect to the Euclidean norm) between either  $\mathbf{x}$  or  $\mathbf{z}$  and low frequency eigenvectors of  $\hat{\Sigma}^{-1}$ . When this occurs, we say that  $\mathbf{x}$  (or  $\mathbf{z}$ ) is spatially smooth with respect to  $\hat{\Sigma}^{-1}$ . Recall, for us, low frequency eigenvectors are those with associated eigenvalues less than 1. We note that (10) is symmetric in  $\mathbf{x}$  and  $\mathbf{z}$ . As just one of these variables becomes more correlated with a low frequency eigenvector, all terms involving it will tend

to decrease in magnitude. Both variables being correlated with low frequency eigenvectors will tend to be associated with a further reduction in the magnitude of the bias. As an illustration, we again use the 140 locations just discussed. We generate a realization  $\mathbf{x}$  from an exponential process ((6) with  $\nu = .5$ ) at these locations with  $\theta = 10$ . In Figure 4c), we illustrate how this realization appears spatially smooth. Because  $\mathbf{x}$  is spatially smooth, it will often be correlated with low frequency eigenvectors. Unsurprisingly, the  $\|\mathbf{x}\|_{\hat{\Sigma}^{-1}}$  is always smaller than the corresponding Euclidean norm. We note that if either  $\mathbf{x}$  or  $\mathbf{z}$  is linearly dependent with  $\mathbf{1}$ , then the bias term in (10) will be 0. Thus, the flatter  $\mathbf{x}$  and  $\mathbf{z}$  become, the smaller the bias.

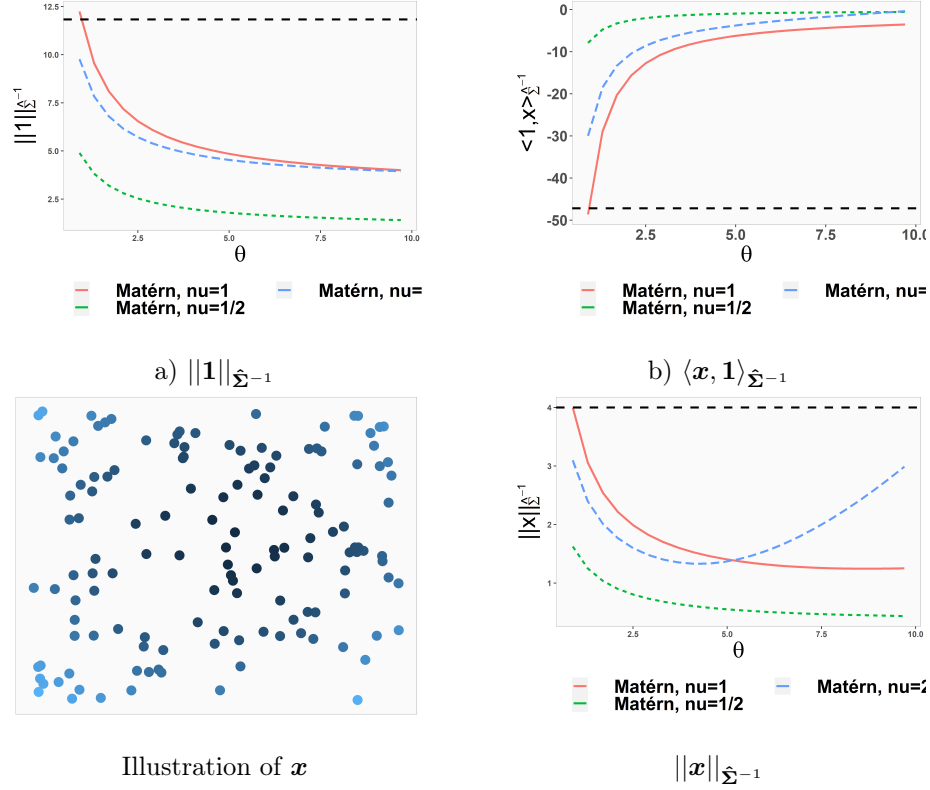


Figure 4: Illustrations of components of (10). All plots were made with Wickham (2016).

The behavior of (10) supports the traditional view that fitting a spatial analysis model helps improve inference on  $\beta_x$ . When the low frequency eigenvectors of  $\hat{\Sigma}^{-1}$  mirrors the patterns of either  $\mathbf{x}$  or  $\mathbf{z}$ , fitting a spatial analysis model will tend to result in better estimates of  $\beta_x$  than a non-spatial model. It also

highlights that what it means to be “spatially smooth” for the purposes of bias reduction depends on the analysis model chosen. To see this, note that in Figure 4 a), b), and d) the magnitudes can be quite different for different choices of  $\hat{\Sigma}^{-1}$ , particularly when  $\theta$  is small.

Recall from our discussion in Section 3.2, researchers are sometimes concerned with collinearity between  $\mathbf{x}$  and  $\mathbf{z}$  as a possible source of confounding bias. We note that when  $\mathbf{z} = \alpha\mathbf{x}$ , for  $\alpha \neq 0$ , then (10) is always less than or equal to  $\alpha\|\mathbf{1}\|_{\hat{\Sigma}^{-1}}^2\|\mathbf{x}\|_{\hat{\Sigma}^{-1}}^2$ . If  $\mathbf{x}$  is correlated with low-frequency eigenvectors or the low-frequency eigenvectors are flat, this term will typically be smaller for a spatial analysis model than for a non-spatial analysis model. In other words, this suggests spatial analysis models can still reduce bias relative to a non-spatial analysis model when  $\mathbf{x}$  or  $\mathbf{z}$  are collinear so long as at least one of them is spatially smooth.

We now turn our attention to the denominator of (8):

$$\begin{aligned} & \|\mathbf{1}\|_{\hat{\Sigma}^{-1}}^2\|\mathbf{x}\|_{\hat{\Sigma}^{-1}}^2 - [\langle\mathbf{x}, \mathbf{1}\rangle_{\hat{\Sigma}^{-1}}]^2 = \\ & \|\mathbf{1}\|_{\hat{\Sigma}^{-1}}^2\|\mathbf{x}\|_{\hat{\Sigma}^{-1}}^2 \sin^2 \phi_{\mathbf{x}, \mathbf{1}}, \end{aligned}$$

where  $\phi_{\mathbf{x}, \mathbf{1}}$  is the angle between  $\mathbf{x}$  and  $\mathbf{1}$  with respect to the Riemannian metric induced by  $\hat{\Sigma}^{-1}$  (see Appendix A for more details). The term  $\sin \phi_{\mathbf{x}, \mathbf{1}}$  will be minimized when  $\mathbf{x}$  is linearly dependent with  $\mathbf{1}$ , and it will be maximized when  $\mathbf{x}$  is perpendicular (with respect to the Riemannian metric induced by  $\hat{\Sigma}^{-1}$ ) to  $\mathbf{1}$ . In other words, because we are considering the denominator of the bias, the flatter  $\mathbf{x}$  becomes, the larger the bias. This behavior supports the insights from research into the analysis model source of spatial confounding:  $\mathbf{x}$  which are “too” spatially smooth *can* distort inference on  $\beta_x$ .

Pulling these insights together, we see that, generally speaking, bias will decrease with a spatial analysis model in settings where  $\mathbf{x}$ ,  $\mathbf{z}$  are spatially smooth or cases in which low frequency eigenvectors of  $\hat{\Sigma}^{-1}$  are flat. We emphasize again that what it means to be spatially smooth depends on the relationship of  $\mathbf{x}$  and  $\mathbf{z}$  with the low frequency eigenvectors of  $\hat{\Sigma}^{-1}$ . However, for cases when  $\mathbf{x}$  is not only spatially smooth, but flat, the numerator and denominator of (8) work in opposite directions. At the extreme, when  $\mathbf{x}$  is collinear with  $\mathbf{1}$ , the bias will be 0 (where we use the mathematical convention that  $\frac{0}{0} = 0$ ). However, as  $\mathbf{x}$  becomes flatter, it’s possible that the denominator will shrink faster than the numerator in some settings. In this case, the flatness of  $\mathbf{x}$  can effectively serve to increase the bias. This reinforces the observations made by researchers influenced by analysis model spatial confounding. Finally, we note that for the case of collinearity between  $\mathbf{x}$  and  $\mathbf{z}$  (i.e., returning to  $\mathbf{z} = \alpha\mathbf{x}$ ,

$\alpha \neq 0$ ), the overall bias term is  $\alpha$  for both spatial analysis models and non-spatial analysis models. This suggests, contrary to some research in data generation spatial confounding, that bias induced by collinearity between  $\mathbf{x}$  and  $\mathbf{z}$  is not exacerbated by fitting a spatial analysis model.

## 4.2 Bias: Adjusted Spatial Analysis Models

In this section, we consider the impact of the analysis model on inference on  $\beta_x$  for the GSEM and Spatial+ approaches referenced in Section 3.3. Recall, these models were developed to improve inference on  $\beta_x$  when certain assumptions about the data generation process are assumed to be true. For the GSEM and Spatial+ methods, these assumptions include that  $\mathbf{x} = \beta_z + \epsilon_x$ . When this is the case, the data generation source of spatial confounding suggests that fitting GSEM or Spatial+ will reduce bias relative to a spatial analysis model or non-spatial analysis model.

We take a moment to give details on both approaches. The GSEM approach, summarized in Adjusted Spatial Analysis Method 1, is equivalent to replacing  $\mathbf{y}$  and  $\mathbf{x}$  with  $\mathbf{r}_y$  and  $\mathbf{r}_x$  (Thaden and Kneib, 2018). This latter set of variables are defined to be the residuals, respectively, from spatial analysis models using  $\mathbf{y}$  and  $\mathbf{x}$  as the response variable with no covariates. These residuals are then used to fit a non-spatial analysis model of the form (2), and inference for  $\beta_x$  is based on the outcome. We note that while Thaden and Kneib (2018) did claim that the GSEM approach is equivalent to these steps, their work did not explore this equivalence. Dupont et al. (2022) utilized the approach for GSEM described in Adjusted Spatial Analysis Method 1 and found that the GSEM approach improved inference only when smoothing was used in Steps 1 and 2, and we adopt this convention from hereon out. The Spatial+ approach, summarized in Adjusted Spatial Analysis Method 2, involves replacing  $\mathbf{x}$  with  $\mathbf{r}_x$ . The analysis model used for inference is then a spatial regression analysis model with response  $\mathbf{y}$  and covariate  $\mathbf{r}_x$ .

**Adjusted Spatial Analysis Method 1 (GSEM).** *The GSEM approach can be summarized as follows:*

1. *Define  $\mathbf{r}_x$  to be the residuals from a spatial regression model with  $\mathbf{x}$  as the response and only an intercept*
2. *Define  $\mathbf{r}_y$  to be the residuals from a spatial regression model with  $\mathbf{y}$  as the response and only an intercept*
3. *Fit an analysis model of the form (2) with response  $\mathbf{r}_y$  and covariate  $\mathbf{r}_x$*

**Adjusted Spatial Analysis Method 2 (Spatial+).** *The Spatial+ approach can be summarized as follows:*

1. Define  $\mathbf{r}_x$  to be the residuals from a spatial regression model with  $\mathbf{x}$  as the response and only an intercept
2. Fit an analysis model of the form (4) with response  $\mathbf{y}$  and covariate  $\mathbf{r}_x$

Both GSEM and Spatial+ can be framed as special cases of adjusted spatial regression analysis models of the form (4). To see this, we assume, unless otherwise stated, that every step of these methods use spatial analysis models of the form (3) (i.e., we use models of the form (3) to find  $\mathbf{r}_y$  and  $\mathbf{r}_x$  in Adjusted Spatial Analysis Method 1 and Adjusted Spatial Analysis Method 2, as outlined in Section 4.2). In Theorem 1, we consider the bias in estimating  $\beta_x$  when  $\mathbf{r}_x$  replaces  $\mathbf{x}$  in a final analysis model.

**Theorem 1.** *Let the data generating model be of the form Equation (1) with  $\mathbf{y}$  and  $\mathbf{x}$  known. We assume that  $\mathbf{r}_x$  are the residuals from a spatial analysis model of the form (4) with response  $\mathbf{x}$  and only an intercept.*

*If the final analysis model is a spatial analysis model of the form (3) with  $\mathbf{x} = \mathbf{r}_x$  and results in the estimate  $\hat{\Sigma}$ , then the bias  $\text{Bias}(\hat{\beta}_x^{AS}) = \beta_x - E(\hat{\beta}_x^{AS})$  can be expressed as:*

$$\beta_z \frac{\left( \|\mathbf{1}\|_{\hat{\Sigma}^{-1}}^2 \langle \mathbf{x}, \mathbf{z} \rangle_{\hat{\Sigma}^{-1}} - \langle \mathbf{x}, \mathbf{1} \rangle_{\hat{\Sigma}^{-1}} \langle \mathbf{z}, \mathbf{1} \rangle_{\hat{\Sigma}^{-1}} \right)}{\|\mathbf{1}\|_{\hat{\Sigma}^{-1}}^2 \|\mathbf{x}\|_{\hat{\Sigma}^{-1}}^2 - [\langle \mathbf{x}, \mathbf{1} \rangle_{\hat{\Sigma}^{-1}}]^2}, \quad (11)$$

*Proof.* See Appendix B.5 for the proof.  $\square$

**Lemma 3.** *If a non-spatial final analysis model of the form (2) is used instead of a spatial analysis model in Theorem 1, then  $\text{Bias}(\hat{\beta}_x^{AS})$  is:*

$$\beta_z \frac{(\|\mathbf{1}\|^2 \langle \mathbf{x}, \mathbf{z} \rangle - \langle \mathbf{x}, \mathbf{1} \rangle \langle \mathbf{z}, \mathbf{1} \rangle)}{\|\mathbf{1}\|^2 \|\mathbf{x}\|^2 - [\langle \mathbf{x}, \mathbf{1} \rangle]^2}. \quad (12)$$

*Proof.* Consider the case when  $\hat{\Sigma}^{-1} = \mathbf{I}$ .  $\square$

The bias for the GSEM method is equivalent to the bias for a non-spatial analysis model (given in (12)). Thus, an immediate insight is that the GSEM approach will result in inference on  $\beta_x$  equivalent to that of a non-spatial analysis using the originally observed  $\mathbf{y}$  and  $\mathbf{x}$ . We note that Dupont et al. (2022) showed, theoretically, that the bias from the GSEM methodology would be equivalent to the bias from a non-spatial model in the context of thin plate

splines when no smoothing occurs. However, their simulations did not find this to be true when smoothing was used. There is a close connection between thin plate splines and mixed models (Ruppert et al., 2003). Here, our mixed model results are most akin to a thin plate spline model where smoothing is used, and thus our results are at odds with those in Dupont et al. (2022). Whereas Dupont et al. (2022)’s simulations suggest that the GSEM methodology would improve inference relative to the spatial model when smoothing is used, our results suggest the opposite. As discussed previously, the non-spatial bias will tend to be larger than the bias from a spatial analysis model when  $\mathbf{x}$  is spatially smooth. Thus, in cases where  $\mathbf{x}$  is spatially smooth, the GSEM method can lead to inferior inference compared to a spatial analysis model.

On the other hand, the bias for the Spatial+ method is of the same form as the bias for a spatial analysis model (given in (11)). All of the discussion involving the behavior of these terms in Section 3.1 are relevant here. Interpreting the impact of performing the Spatial+ method relative to the performance of a spatial analysis model is difficult, however. For example, consider comparing the Spatial+ method to the spatial analysis model employed in step 2 of Adjusted Spatial Analysis Method 2. The difference between using  $\mathbf{r}_\mathbf{x}$  and  $\mathbf{x}$  in this spatial analysis model boils down to the estimated  $\hat{\Sigma}^{-1}$ . If  $\mathbf{r}_\mathbf{x}$  is defined to the residuals from a spatial analysis model of the form (3), then  $\mathbf{r}_\mathbf{x} = \mathbf{x} - \delta \mathbf{1}$  for  $\delta \geq 0$ . The fact that  $\mathbf{r}_\mathbf{x}$  is a translation of  $\mathbf{x}$  suggests that the estimated covariances will likely be similar when the analysis uses a positive-definite covariance structure (we would expect the largest difference to be in the estimation of  $\beta_0$ ). This insight will not necessarily hold for models employing GMRF’s, where the precision is non-singular. Proving these insights theoretically is difficult. We rely on simulation studies in Section 5 to explore these ideas more thoroughly. If these intuitions hold, however, then the Spatial+ method will yield almost equivalent inference as a traditional spatial analysis model with positive-definite covariance structures.

Importantly, we emphasize these results suggest adjusted spatial analysis models will not improve inference for regression coefficients even in the settings they are designed to be used in when spatial linear mixed models are used to fit them.

## 5 Simulation Studies

In all of the following simulation studies, we consider settings that have been identified in the literature as times when spatial confounding can distort



inference for a regression coefficient. For each of these settings, we consider the absolute value of the bias for a regression coefficient for non-spatial, spatial, and adjusted spatial analysis models. Each simulation study is designed to explore whether insights from analysis model spatial confounding explored in Section 3.1 or the data generation spatial confounding explored in Section 3.2 have any relevance to the patterns of bias observed for estimates of regression coefficients.

The results of this paper have primarily focused on spatial linear mixed models that involve positive-definite covariance structures. However, the intrinsic conditional autoregressive (ICAR) model plays an important role in the spatial confounding literature. It was the model first considered in Hodges and Reich (2010) and Reich et al. (2006) in the modern introduction to the phenomena of spatial confounding. As referenced previously, the Spatial + methodology was originally developed for the thin spline plate setting, but the authors stated that the methodology should extend to the ICAR model (Besag et al., 1991). The methodology in Thaden and Kneib (2018) was also originally proposed for areal data where the ICAR model is traditionally used, and the spatial model these authors considered is thought to be equivalent to the ICAR model. Thus, in these simulation studies, we consider both geostatistical data fit to the class of models considered in our results (referred to as the “Geostatistical data setting”) as well as areal data fit to an ICAR model (referred to as the “Areal data setting” because the ICAR model employs a GRMF).

Because we have not previously defined the ICAR model before, we take a moment to do so here. The ICAR model incorporates spatial dependence for areal data with the introduction of an underlying, undirected graph  $G = (V, E)$ . Non-overlapping spatial regions that partition the study area are represented by vertices,  $V = \{1, \dots, n\}$ , and edges  $E$  defined so that each pair  $(i, j)$  represents the proximity between region  $i$  and region  $j$ . We represent  $G$  by its  $n \times n$  binary adjacency matrix  $\mathbf{A}$  with entries defined such that  $\text{diag}(\mathbf{A}) = 0$  and  $\mathbf{A}_{i,j} = \mathbb{1}_{(i,j) \in E, i \neq j}$ . The ICAR model could be considered a generalization of the spatial analysis model of the form (3), by stating that the spatial random effect has a distribution proportional to a multivariate normal distribution with mean  $\mathbf{0}$  and precision matrix  $\tau^2 (\mathbf{I}\mathbf{A}\mathbf{1} - \mathbf{A}) = \tau^2 \mathbf{Q}$ , where  $\tau^2$  controls the rate decay for the spatial dependence and  $\mathbf{Q}$  is the graph Laplacian.

This precision matrix is not of full rank, so we use a Bayesian analysis to fit all the relevant spatial models. We note there is a close connection between certain types of Bayesian analysis in this setting and modeling spatial random effects through the use of a smoothing penalty, as is done in the thin plate

spline setting (Dupont et al., 2022; Rue and Held, 2005; Kimeldorf and Wahba, 1970). Because the graphs we consider are connected, there is an implicit intercept present in the ICAR model (Paciorek, 2009). Therefore, we omit an intercept from our spatial analysis models. For a Bayesian analysis,  $\sigma^2$  and  $\tau^2$  require priors. Here, we give them Inverse-Gamma distributions with scale and rate .01 each. Finally, to make the non-spatial model comparable, we also use a Bayesian analysis, giving the  $\sigma^2$  parameter an Inverse-Gamma prior with the same hyperparameters as the spatial model. All models are fit with using Markov Chain Monte Carlo (MCMC) algorithms with Gibbs updates. All MCMC's are run for 80,000 iterations with a 20,000 burn-in.

## 5.1 Non-spatial and Spatial Analysis Models

In this sub-section, we use simulation studies to compare a spatial and non-spatial model. For the spatial linear mixed model setting, we simulate data to ensure that spatial confounding from a data generation perspective is present. For the Gaussian Markov Random Field setting, we simulate data to ensure that spatial confounding from an analysis model setting is present.

### 5.1.1 Geostatistical Data Setting

In this subsection, we simulate data to replicate the setting explored in Section 3.2. The data are all generated from a model of the form (1) as follows:

$$\mathbf{y}_i = 0.3 + \mathbf{x}_i + 2\mathbf{z}_i + \epsilon_i,$$

where  $\epsilon_i$  are independently simulated from a normal distribution with mean 0 and variance 0.1.

The 200 locations of the data are randomly generated on  $[0, 10] \times [0, 10]$  window one time, and these locations are then held fixed. The realizations  $\mathbf{x}$  and  $\mathbf{z}$  are simulated from mean zero spatial processes, denoted respectively  $\mathbf{X}$  and  $\mathbf{Z}$ , with spatial covariance structures defined by  $C(d, \theta) = 0.1 \exp\{\frac{-h}{\theta}\}$  for euclidean distance  $h$  (i.e., the exponential field).

We define  $\mathbf{X} = \mathbf{X}_c + \mathbf{X}_u$  and  $\mathbf{Z}$  as follows:  $\text{Cov}(\mathbf{X}) = \mathbf{C}(\theta_c) + \mathbf{C}(\theta_u)$ ,  $\text{Cov}(\mathbf{Z}) = \mathbf{C}(\theta_c)$ , and  $\text{Cov}(\mathbf{X}, \mathbf{Z}) = \rho\mathbf{C}(\theta_c)$ . We generate 1000 datasets for each  $(\theta_u, \theta_c, \rho) \in \{1, 5, 10\} \times \{1, 5, 10\} \times \{-.9, -.6, -.3, 0, .3, .6, .9\}$ . For each dataset, we then fit a non-spatial analysis model of the form (2) and a spatial analysis model of the form (3). For the latter,  $g()$  is assumed to have spatial structure defined by  $C(d, \theta) = \sigma_s^2 \exp\{\frac{-h}{\theta}\} + \sigma_e^2 \mathbf{I}$ , with unknown  $\theta$ ,  $\sigma_s^2$ , and  $\sigma_e^2$ . Both analysis models are fit via residual maximum likelihood (REML).

We consider the absolute value of the bias for  $\beta_x$  for both the non-spatial and spatial analysis models. Recall from Section 3.2 that many researchers use results from Paciorek (2010) (visualized in Figure 2) to support statements that fitting a spatial analysis model will lead to increased bias whenever  $\theta_c \ll \theta_u$ . In Figure 4, we can see that the absolute bias tends to be larger for non-spatial models than for spatial models for all possible combinations for  $\theta_c$  and  $\theta_u$ . These results support our findings in Section 3.1 (as well as findings in Section 2.1 of Paciorek (2009) regarding a spatial model fit via REML) that spatial analysis models will tend to reduce bias relative to non-spatial models. The discrepancy may simply be due to the fact that Paciorek (2009)’s original observation was made about a different type of spatial structure. However, when we repeated his results for the exponential spatial structure used here (visualized in Figure 3), the data generation focus on spatial confounding suggested that bias for spatial analysis models would increase (relative to non-spatial models) when  $\theta_c < 2$ . However, this did not appear to be true here in these simulations. Importantly, this is evidence that focusing on the data generation source of spatial confounding alone may not be able to explain bias in regression coefficients.

Of course, Figure 5a) considers how bias behaved across all datasets. If we compare the absolute value of the bias from a non-spatial analysis model and a spatial analysis model for a fixed dataset, the spatial analysis model resulted in less bias approximately 72% of the time. This remained true across all possible combinations of  $\theta_c$  and  $\theta_u$  (with the percentage of times the spatial bias was preferable varying from 62% to 77%). There did not appear to be a strong relationship in the patterns of bias as a function of  $\rho$ .

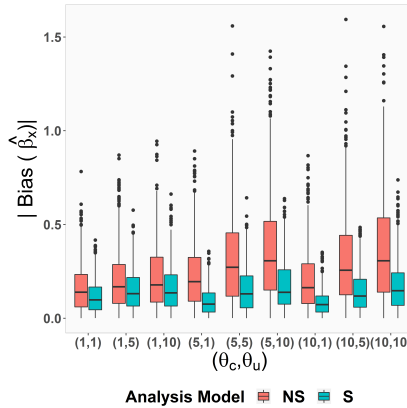


Figure 5: Boxplots of the absolute value of the observed bias i.e.,  $|\text{Bias}(\hat{\beta}_x)|$ . Plot made with `ggplot2` Wickham (2016).

Across all combinations of  $\theta_c$  and  $\theta_u$ , the maximum absolute bias observed for the spatial model was 0.74. On the other hand, the maximum absolute bias for the non-spatial model was 1.6, and approximately 1.1% of the time the non-spatial analysis model resulted in an absolute value of bias over 1. To get a feel for the more general trends, we consider cases in which the bias for an analysis model accounted for over a 25% change in  $\beta_x$  (i.e., when  $\left|\frac{\hat{\beta}_x - \beta_x}{\beta_x}\right| > .25$ ). Such cases occurred approximately 15% of the time for the spatial analysis model and 42% of the time for the non-spatial model. When these more extreme cases of bias occurred for the spatial analysis model tended to vary across particular combinations of  $\theta_u$  and  $\theta_c$ . In particular when  $\theta_u$  is 1, the bias from a spatial analysis model accounted for a 25% change in estimates  $\beta_x$  less frequently (less than 1% of the time) compared to over 20% of the time for cases when  $\theta_u > 1$ . The insight for data generation spatial confounding were not particularly relevant in predicting the performance (with respect to absolute bias) for the spatial analysis model.

In summary, these results suggest that, on average, in the presence of either a spatially smooth  $\mathbf{x}$  or residual spatial dependence ( $\mathbf{z}$ ), a spatial analysis model will result in less bias than the a non-spatial analysis model. Perhaps more importantly, the magnitude of the bias when things go wrong is much larger for the non-spatial analysis model than the spatial analysis model. We emphasize that these results suggest that the spatial analysis model outperforms the non-spatial analysis model in settings where the data generation spatial confounding focus suggests the opposite should happen.

### 5.1.2 Areal Data Setting

In the second setting, we work with areal data on an  $11 \times 11$  grid on the unit square. Recall, work in analysis model spatial confounding suggest that a covariate which is collinear with low-frequency eigenvectors of the precision matrix of the spatial random effect could induce bias in the estimation of  $\beta_x$ . This is thought to be true regardless of whether there is a “missing” spatially dependent covariate. Here, we attempt to explore whether that is the case by simulating datasets with both a spatially-smooth covariate and with a covariate without much spatial structure.

For all simulated datasets, the response  $\mathbf{y}$  is generated from a model of the

form (1) as follows:

$$\mathbf{y}_i = 0.3 + 3\mathbf{x}_i + \boldsymbol{\epsilon}_i,$$

where each  $\epsilon_i$  is independently distributed from a normal distribution with mean 0 and variance 1. We explicitly leave out any residual spatial dependence from the data generation model in order to explore the impact of a covariate alone.

We consider two possible choices of  $\mathbf{x}$ : one in which  $\mathbf{x}$  is spatially-smooth from an analysis model spatial confounding perspective and one in which it is not. For the latter category, we simply generate  $\mathbf{x}$  from a normal distribution with mean 0 and variance  $\sqrt{0.6}$  once, as depicted in the left plot of Figure 6. We hold this vector fixed and simulate the response variable 100 times. In order to generate the spatially-smooth covariate we use the eigenvectors of the graph Laplacian  $\mathbf{Q}$ . For the ICAR model, there is not a variance-covariance matrix, but rather the singular precision matrix. However, we can treat this as the pseudo-inverse of a variance-covariance matrix (Paciorek, 2009). In this case, then, if  $\mathbf{x}$  is strongly correlated with a low-frequency eigenvector of  $\mathbf{Q}$ , the spatial analysis model may perform more poorly than the non-spatial model. Thus, we let  $\mathbf{x}$  to be the eigenvector of  $\mathbf{Q}$  associated with smallest, non-zero eigenvalue, depicted in the right plot of Figure 6. As before, we hold this vector fixed for 100 simulated datasets.

For each of the 200 datasets, we consider 2 analysis models: 1) a non-spatial analysis model, and 2) a spatial analysis model. Here, the spatial analysis models is the ICAR model. We use a Bayesian approach for both the spatial and the non-spatial analysis models, as described in the introduction of this section.

When  $\mathbf{x}$  is not spatially smooth (i.e., randomly generated from a normal distribution), the spatial analysis and non-spatial analysis models gave relatively similar inferences for  $\beta_x$ . In the left hand plot of Figure 7, we see that across datasets, the absolute bias was relatively similar for both analysis models. In the right hand plot of Figure 7, we see that for individual datasets, the inference was also fairly similar for the two analysis models as well. In this plot, the absolute bias for the spatial analysis model is on the x-axis and the absolute bias for the non-spatial analysis model is on the y-axis. Datasets for which the covariate is not spatially smooth are colored red. The black dashed line represents when the spatial and non-spatial analysis models had equivalent bias; while the gray dashed lines represent where the absolute bias differed by 1 between the analysis models. A triangular shape indicates that the spatial analysis model had a smaller absolute bias than the non-spatial analysis model. The spatial model resulted in less absolute bias 49% of the time.

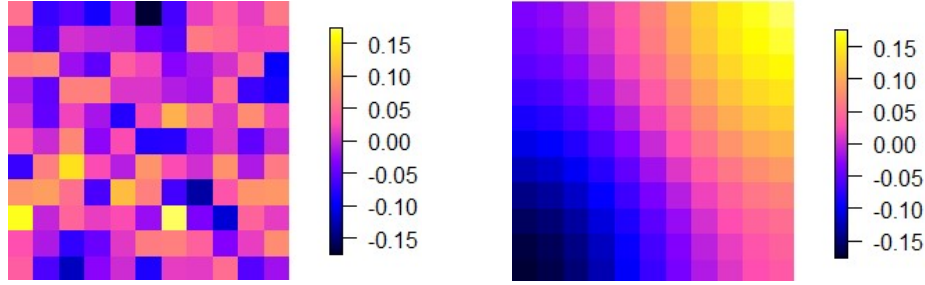


Figure 6: Visualization of a)  $\mathbf{x}$  generated from a normal distribution (“random”), b)  $\mathbf{x}$  defined as the low-frequency eigenvector of  $\mathbf{Q}$  (“spatially smooth”). Plots made with **raster** package (Hijmans, 2022).

When  $\mathbf{x}$  is spatially smooth (i.e., it is the low frequency eigenvector of  $\mathbf{Q}$ ), the story does change a bit. In the left hand plot of Figure 7, we see that across datasets, the absolute bias of the spatial model has a slightly more right-skewed distribution. In the right hand plot of Figure 7, we see that for individual datasets, the inference was still fairly similar for the two analysis models. In this plot, recall, the absolute bias for the spatial analysis model is on the x-axis and the absolute bias for the non-spatial analysis model is on the y-axis. Datasets for which the covariate is spatially smooth are colored blue. The spatial model resulted in less absolute bias 39% of the time.

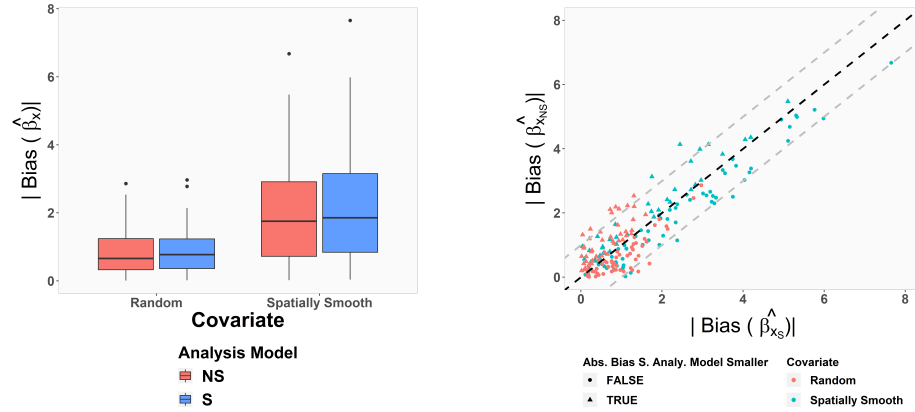


Figure 7: On the left, we see boxplots of the absolute bias for the spatial and non-spatial analysis models. On the right, the points are individual simulated datasets with the absolute bias from the spatial analysis model on the x-axis and absolute bias from the non-spatial analysis model on the y-axis. Plots made with **ggplot2** package (Wickham, 2016).

In sum, there is evidence that a spatially-smooth covariate (i.e., one correlated with a low frequency eigenvector of the graph Laplacian in this setting) may cause the spatial analysis model to have higher absolute bias than the non-spatial analysis model. However, the impact may not be particularly large in magnitude. Here we considered a covariate that was perfectly correlated with the eigenvector associated with the smallest (non-zero) eigenvalue. This is essentially a worst-case scenario, and the spatial analysis model and non-spatial analysis models still yielded similar inference. In fact, as seen in Figure 7, when the absolute bias for the non-spatial and spatial model differed by more than 1, the non-spatial model tended to have the higher absolute bias.

## 5.2 Spatial Analysis and Adjusted Spatial Analysis Models

In this sub-section, we generate data to replicate the setting explored in (Thaden and Kneib, 2018) and (Dupont et al., 2022). For the geostatistical data setting, we seek to explore whether a spatial analysis model of the form (3) induces more bias than two adjusted spatial analysis models of the form (4). We restrict our attention to the Spatial Linear Mixed Model setting, as the impropriety of the ICAR model would require careful consideration of how to define a residual in a model with no covariates.

### 5.2.1 Geostatistical Data Setting

In this setting, the 400 locations of the data are randomly generated on  $[0, 10] \times [0, 10]$  window one time, and these locations are then held fixed throughout the subsequent simulations. Thaden and Kneib (2018) and Dupont et al. (2022) studied similar set-ups. Both papers considered settings in which:

$$\mathbf{x} = 0.5\mathbf{z} + \epsilon_x.$$

Thaden and Kneib (2018) chose  $\mathbf{z}$  to be fixed to three possible spatial patterns. Dupont et al. (2022) generated  $\mathbf{z}$  from an exponential process (i.e., a spatial structure of the form (6) with  $\nu = .5$ ) with  $\theta = 5$  and then replaced  $\mathbf{z}$  with the fitted values of a spatial thin plate regression spline fitted to it. This approach was meant to ensure that both the response variable and the covariates can be described by thin splines, and therefore eliminate bias due to model misspecification. Their supplemental materials suggested simply using the Gaussian processes yielded similar results, though (see Web Appendix F of Dupont et al. (2022)). Because we find covariates defined to be the fitted values

from a thin plate spline to be very restrictive, we adopt the convention of the supplemental material from Dupont et al. (2022) here (i.e., a spatial structure of the form (6) with  $\nu = .5$  and  $\theta = 5$ ). We chose  $\epsilon_x$  to be independently distributed from a normal with mean 0 and variance  $\sigma_x^2 = 0.1$ . The response  $\mathbf{y}$  is generated from a model of the form (1) as follows:

$$\mathbf{y}_i = 0.3 + 2\mathbf{x}_i - \mathbf{z}_i + \epsilon_i,$$

where  $\epsilon_i$  are independently generated from a normal distribution with mean 0 and variance  $\sigma_y^2 = 0.1$ .

We consider 4 analysis models: 1) a non-spatial analysis model of the form (2) (“NS”), 2) a spatial analysis model of the form (4) (“S”), 3) the GSEM adjusted spatial analysis model, and 4) a Spatial+ adjusted spatial analysis model. All models are fit with REML and the spatial random effects are all represented with a spatial structure defined by  $C(d, \theta) = \sigma_s^2 \exp\{\frac{-h}{\theta}\} + \sigma_e^2 \mathbf{I}$ , with unknown  $\theta$ ,  $\sigma_s^2$ , and  $\sigma_e^2$ .

As predicted in Section 4.2, the GSEM model yields the same inference as the non-spatial analysis model for all simulated datasets. Similarly, the Spatial+ model yields essentially the same observed biases as the spatial analysis model. In Figure 8a) we plot the absolute value for the observed bias across all analysis models. The spatial analysis model and Spatial+ model tend to result in significantly less bias than the GSEM and non-spatial model. We note that for a fixed data set, the spatial analysis model always produced less bias than the non-spatial and GSEM.

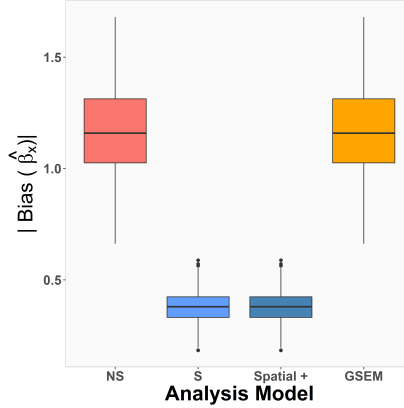


Figure 8: Boxplots of the absolute value of the observed bias, All plots were made with Wickham (2016).



In summary, we find that even if there is high collinearity between  $\mathbf{x}$  and  $\mathbf{z}$ , the spatial linear mixed model significantly improves inference on  $\beta_x$  relative to a non-spatial model. Additionally, the GSEM and Spatial+ methodologies in this context do not improve inference for  $\beta_x$ . Importantly, this again illustrates that insights from a data generation perspective of spatial confounding may not be particularly useful in explaining the patterns of bias.

### 5.3 Approaches for Fitting Adjusted Spatial Analysis Models

The Spatial+ and the GSEM models were proposed in papers that did not utilize spatial linear mixed models in simulation studies. Instead, both considered spatial analysis models that fit with the R package `mgcv`. The Spatial+ method employed thin plate splines, while the GSEM model utilized a smoothing penalty that is supposed to be equivalent to the ICAR model. In this subsection, we consider both the geostatistical data setting and the areal data setting and we now we fit our spatial models with the `mgcv` package, utilizing thin plate splines as in Dupont et al. (2022).

#### 5.3.1 Geostatistical Data Setting

Here, we simulate data exactly as in Section 5.2. We explore fitting 4 analysis models. The first three are: 1) a spatial analysis model (“S PS”), 2) A GSEM analysis model (“GSEM PS”), and 3) a Spatial+ model (“Spatial + PS”). We fit all associated spatial models with the default settings of the `mgcv` package as in Thaden and Kneib (2018) and Dupont et al. (2022). The default settings involve using penalized thin plate splines. We note that manual increases of the number of knots did not substantially change results for a simulated dataset, so we simply used the default selections. For comparison, we include the fourth analysis model (“S”). This is the same spatial analysis model considered in Section 5.2 fit via REML.

We plot the absolute value of the biases for all analysis models in Figure 9. If we only considered models fit with the `mgcv` package, we note that both the Spatial+ and GSEM analysis models tend to have slightly smaller bias than the spatial model. However, the spatial analysis model fit via REML outperforms all models.

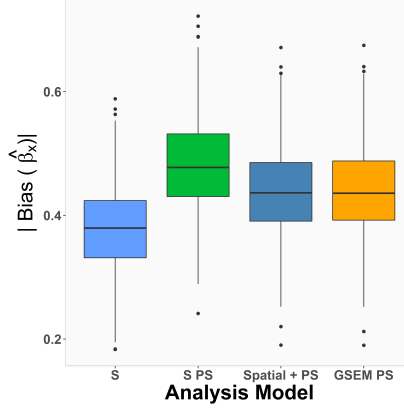


Figure 9: Boxplots of the absolute value of the observed bias. Plot made with the `ggplot2` package (Wickham, 2016).

This suggests, as did our results in Section 3.1 and Section 3.3, that collinearity between  $\mathbf{x}$  and  $\mathbf{z}$  is not necessarily problematic in the spatial linear mixed model setting. In fact, relative to both a non-spatial model (explored in Section 5.2) and the two adjusted spatial analysis models here, the spatial analysis model is the best at reducing absolute bias for estimates of  $\beta_x$ . In the context of the broader literature, we note the finding that the Spatial + and GSEM improve inference relative to a penalized thin plate splines agrees with the simulation results in Spatial +. In other words, it's possible that the smoothing in this setting in combination with collinearity between  $\mathbf{x}$  and  $\mathbf{z}$  may increase absolute bias in the estimates for  $\beta_x$ . This problem may be mitigated by the Spatial + and GSEM approaches, however, still results in increased bias relative to a spatial linear mixed model.

### 5.3.2 Areal Data Setting

In the second setting, we work with areal data on an  $11 \times 11$  grid on the unit square as in Section 5.1.2. Following the simulation studies in Thaden and Kneib (2018), we hold  $\mathbf{z}$  fixed for the generation of all data. We then define the rest of the model as in Thaden and Kneib (2018) as follows:

$$\mathbf{x} = 0.5\mathbf{z} + \epsilon_x,$$

where  $\epsilon_x$  is independently distributed from a normal distribution with mean 0 and variance  $\sigma_x^2$ . The response  $\mathbf{y}$  is generated from a model of the form (1) as follows:

$$\mathbf{y}_i = 0.3 + 3\mathbf{x}_i - \mathbf{z}_i + \epsilon_i,$$

where each  $\epsilon_i$  is independently distributed from a normal distribution with mean 0 and variance  $\sigma_y^2$ . In Thaden and Kneib (2018), the authors observed the largest differences between the GSEM analysis model and the spatial analysis model for  $(\sigma_x, \sigma_y) = \{(0.15, 1), (0.15, 0.15)\}$ . We consider these two settings, and choose  $\mathbf{z}$  to be the eigenvector of  $\mathbf{Q}$  associated with the smallest non-zero eigenvalue as in Section 5.1.2 (depicted in Figure 6b). We choose this value to allow for some comparisons to our findings in Section 5.1.2. Although we note the exact  $\mathbf{x}$  and its sample variance will be, of course, different,  $\mathbf{x}$  will still tend to be highly collinear with the lowest frequency eigen-vector of the graph Laplacian.

For both combinations of  $(\sigma_x, \sigma_y)$ , we simulate 100 datasets for analysis. We consider four analysis models. The first three are again: 1) a spatial analysis model (“S PS”), 2) A GSEM analysis model (“GSEM PS”), and 3) a Spatial+ model (“Spatial + PS”). All these models are again fit with the `mgcv` package, utilizing thin plate splines as in Section 5.3.1. For comparisons, we also consider the ICAR model (“S”). In Figure 10, we summarize the results for the absolute bias. The absolute bias, unsurprisingly, increases for all analysis models as the  $\frac{\sigma_x}{\sigma_y}$  decreases. For both combinations of  $(\sigma_x, \sigma_y)$ , the ICAR analysis model tends to have the smallest absolute bias followed by the penalized thin plate analysis model. The GSEM and Spatial+ analysis models gave similar inferences, and tended to be higher than either of the unadjusted spatial models.

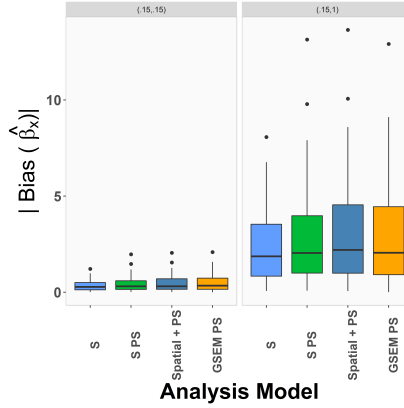


Figure 10: Boxplots of the absolute value of the observed bias. On the left hand side  $(\sigma_x, \sigma_y) = (0.15, 0.15)$ , and on the right hand side  $(\sigma_x, \sigma_y) = (0.15, 1)$ . Plot made with the `ggplot2` package (Wickham, 2016).

We take a moment to compare our results from the ICAR analysis model here to the ICAR analysis model in Section 5.1.2. Here, the setting most similar to that in the previous section is when  $\sigma_y = 1$ , and in both simulation studies the

bias we observe is very similar. For example, here the mean of the absolute biases was approximately 2.4 and the median of the absolute biases was approximately 1.9. In Section 5.1.2, the mean of the absolute biases was approximately 2.1 and the median was approximately 1.9. Recall, in Section 5.1.2, there was no missing confounder ( $\mathbf{z}$ ) or residual spatial dependence in the data generation model. For the ICAR analysis model, the fact that we observe similar bias patterns in Section 5.1.2 and Section 5.3.2 offers evidence that the collinearity between  $\mathbf{x}$  and  $\mathbf{z}$  is not the sole source of the bias we observe here. Instead, it would seem the collinearity between  $\mathbf{x}$  and the Graph Laplacian is the primary driver of bias.

We note that the fact that the Spatial+ and GSEM approaches yield larger absolute biases (although the differences are not huge) than either the ICAR analysis model or the penalized thin plate splines directly contradicts the findings in Thaden and Kneib (2018) and Dupont et al. (2022). This offers, at least, some evidence that these approaches may not be entirely appropriate in the Bayesian context.

## 6 Discussion

In this paper, we have synthesized the broad, and often muddled, literature on spatial confounding. We have introduced two broad focuses in the spatial confounding literature: the analysis model focus and the data generation focus. Using the spatial linear mixed model, we have shown how papers focused on the former category often conceptualize the problem of spatial confounding as originating from the relationship between an observed covariate  $\mathbf{x}$  and the estimated precision matrix  $\hat{\Sigma}_g^{-1}$  of a spatial random effect. We then showed how papers focused on the latter category typically identify the problem of spatial confounding as originating from the relationship between an observed covariate ( $\mathbf{x}$ ) and a collinear, unobserved covariate ( $\mathbf{z}$ ).

Our results highlight two important conclusions: 1) the original conceptualization of spatial confounding as “problematic” may not have been entirely correct, and 2) the analysis model and data generation perspectives of spatial confounding can lead to directly contradictory conclusions about whether spatial confounding exists and whether it adversely impacts inference on regression coefficients. With respect to the first point, the modern conceptualization of spatial confounding arose in work by Reich et al. (2006) and Hodges and Reich (2010). In our proposed framework, these papers focused on an analysis model type of spatial confounding. In the context of an ICAR model,

they argued that whenever  $\mathbf{x}$  was collinear with a low-frequency eigenvector of the graph Laplacian  $\mathbf{Q}$ , the regression coefficients would be biased (relative the regression coefficients obtained from a non-spatial model). Our results suggest, that, in general, collinearity between  $\mathbf{x}$  and low-frequency eigenvectors of the graph Laplacian helps to *reduce* bias in regression coefficients. It is only in relatively extreme cases, where  $\mathbf{x}$  is “flat” and there is no spatially smooth residual dependence that bias for regression coefficients can increase. In our simulation study, we produced such a setting by generating  $\mathbf{x}$  to be perfectly correlated with a low frequency eigenvector of the graph Laplacian. Even in this extreme scenario, however, the bias seen in a spatial analysis model was not that much different from the bias seen in a non-spatial analysis model.

Turning our attention to the second point, the data generation perspective of spatial confounding often relies on very specific assumptions about the processes that generated  $\mathbf{x}$  and  $\mathbf{z}$  or on very specific assumptions about the relationship between these variable (i.e.,  $\mathbf{x}$  is a combination of  $\mathbf{z}$  and some Gaussian noise). Our results suggested that many of the scenarios that are identified as problematic from a data generation perspective are not problematic (at all) from an analysis model perspective. This is potentially problematic because many of these papers propose methods to “alleviate” spatial confounding based on the perceived problem (the relationship between  $\mathbf{x}$  and  $\mathbf{z}$ ). In our simulation studies, we studied scenarios identified in the literature as being problematic from a data generation focus on spatial confounding. We considered two settings: a geostatistical data setting and an areal data setting. For the geostatistical data setting, a spatial analysis model fit with REML tended to outperform a non-spatial analysis model in all cases. Additionally, this spatial model either outperformed or was equivalent to the inference derived from adjusted spatial analysis models. For the areal data setting, we found that the adjusted spatial analysis models increased the absolute bias relative to two types of spatial analysis model. In other words, focusing on the relationship between  $\mathbf{x}$  and  $\mathbf{z}$  (or the processes that generated them) did not help identify settings where a spatial analysis model distorted inference. Using these insights to “adjust” for spatial confounding lead to inferences on regression coefficients that were worse than a standard spatial analysis model.

Taken together, the results and simulation studies in this paper offer support for conventional wisdom of spatial statistics: accounting for residual spatial dependence tends to improve inference on regression coefficients. However, spatial analysis models are not interchangeable: the analysis model *and the method used to fit it* matter. For example, Dupont et al. (2022) correctly

identified settings in which collinearity between  $\boldsymbol{x}$  and  $\boldsymbol{z}$  could lead to bias when penalized thin plate splines were used. In those settings, the Spatial+ methodology does reduce bias relative to the spatial penalized thin plate splines model. However, a spatial linear mixed model fit via REML outperforms both of these models with respect to bias. Importantly, the Spatial+ methodology did not continue to improve inference for a Bayesian approach. In order to avoid the pitfalls that currently plague the field of spatial confounding, future work motivated by spatial confounding needs to be more careful to both precisely define what is being studied and the analysis model being utilized.

## References

- [1] Adin, A., Goicoa, T., Hodges, J. S., Schnell, P. M., and Ugarte, M. D. (2021). Alleviating confounding in spatio-temporal areal models with an application on crimes against women in india. *Statistical Modelling*, page 1471082X211015452.
- [2] Azevedo, D. R., , M. O., and Bandyopadhyay, D. (2021). Mspock: Alleviating spatial confounding in multivariate disease mapping models. *Journal of Agricultural, Biological and Environmental Statistics*, pages 1–28.
- [3] Azevedo, D. R., Prates, M. O., and Bandyopadhyay, D. (2022). Alleviating spatial confounding in frailty models. *Biostatistics*.
- [4] Besag, J., York, J., and Mollié, A. (1991). Bayesian image restoration, with two applications in spatial statistics. *Annals of the institute of statistical mathematics*, 43(1):1–20.
- [5] Bivand, R. S., Pebesma, E. J., Gómez-Rubio, V., and Pebesma, E. J. (2008). *Applied spatial data analysis with R*, volume 747248717. Springer.
- [6] Chiou, Y.-H., Yang, H.-D., and Chen, C.-S. (2019). An adjusted parameter estimation for spatial regression with spatial confounding. *Stochastic Environmental Research and Risk Assessment*, 33(8):1535–1551.
- [7] Clayton, D. G., Bernardinelli, L., and Montomoli, C. (1993). Spatial correlation in ecological analysis. *International Journal of Epidemiology*, 22(6):1193–1202.
- [8] Cressie, N. (1993). *Statistics for Spatial Data*. Wiley.
- [9] Diggle, P. J., Tawn, J., and Moyeed, R. (1998). Model-based geostatistics. *Journal of the Royal Statistical Society: Series C (Applied Statistics)*, 47(3):299–350.
- [10] Douglas Nychka, Reinhard Furrer, John Paige, and Stephan Sain (2021). fields: Tools for spatial data. R package version 14.0.
- [11] Dupont, E., Wood, S. N., and Augustin, N. H. (2022). Spatial+: a novel approach to spatial confounding. *Biometrics*.
- [12] Hanks, E. M., Schliep, E. M., Hooten, M. B., and Hoeting, J. A. (2015). Restricted spatial regression in practice: geostatistical models, confounding, and robustness under model misspecification. *Environmetrics*, 26(4):243–254.

- [13] Hefley, T. J., Hooten, M. B., Hanks, E. M., Russell, R. E., and Walsh, D. P. (2017). The bayesian group lasso for confounded spatial data. *Journal of Agricultural, Biological and Environmental Statistics*, 22(1):42–59.
- [14] Hijmans, R. J. (2022). *raster: Geographic Data Analysis and Modeling*. R package version 3.5-15.
- [15] Hodges, J. S. and Reich, B. J. (2010). Adding spatially-correlated errors can mess up the fixed effect you love. *The American Statistician*, 64(4):325–334.
- [16] Hughes, J. and Haran, M. (2013). Dimension reduction and alleviation of confounding for spatial generalized linear mixed models. *Journal of the Royal Statistical Society: Series B (Statistical Methodology)*, 75(1):139–159.
- [17] Hui, F. K. and Bondell, H. D. (2021). Spatial confounding in generalized estimating equations. *The American Statistician*, pages 1–10.
- [18] Keller, J. P. and Szpiro, A. A. (2020a). Selecting a scale for spatial confounding adjustment. *Journal of the Royal Statistical Society: Series A (Statistics in Society)*, 183(3):1121–1143.
- [19] Keller, J. P. and Szpiro, A. A. (2020b). Selecting a scale for spatial confounding adjustment. *Journal of the Royal Statistical Society. Series A, (Statistics in Society)*, 183(3):1121.
- [20] Kelling, C., Graif, C., Korkmaz, G., and Haran, M. (2021). Modeling the social and spatial proximity of crime: domestic and sexual violence across neighborhoods. *Journal of quantitative criminology*, 37(2):481–516.
- [21] Khan, K. and Calder, C. A. (2020). Restricted spatial regression methods: Implications for inference. *Journal of the American Statistical Association*, pages 1–13.
- [22] Kimeldorf, G. S. and Wahba, G. (1970). Spline functions and stochastic processes. *Sankhyā: The Indian Journal of Statistics, Series A*, pages 173–180.
- [23] Marques, I., Kneib, T., and Klein, N. (2022). Mitigating spatial confounding by explicitly correlating gaussian random fields. *Environmetrics*, page e2727.
- [24] Nobre, W. S., Schmidt, A. M., and Pereira, J. B. (2021). On the effects of spatial confounding in hierarchical models. *International Statistical Review*, 89(2):302–322.



- [25] Paciorek, C. (2009). Technical vignette 5: Understanding intrinsic gaussian markov random field spatial models, including intrinsic conditional autoregressive models. *Technical report*.
- [26] Paciorek, C. J. (2010). The importance of scale for spatial-confounding bias and precision of spatial regression estimators. *Statistical Science: A Review Journal of the Institute of Mathematical Statistics*, 25(1):107.
- [27] Page, G. L., Liu, Y., He, Z., and Sun, D. (2017). Estimation and prediction in the presence of spatial confounding for spatial linear models. *Scandinavian Journal of Statistics*, 44(3):780–797.
- [28] Papadogeorgou, G., Choirat, C., and Zigler, C. M. (2019). Adjusting for unmeasured spatial confounding with distance adjusted propensity score matching. *Biostatistics*, 20(2):256–272.
- [29] Prates, M. O., Assuncao, R. M., and Rodrigues, E. C. (2019). Alleviating spatial confounding for areal data problems by displacing the geographical centroids. *Bayesian Analysis*, 14(2):623–647.
- [30] Reich, B. J. and Hodges, J. S. (2008). Identification of the variance components in the general two-variance linear model. *Journal of Statistical Planning and Inference*, 138(6):1592–1604.
- [31] Reich, B. J., Hodges, J. S., and Zadnik, V. (2006). Effects of residual smoothing on the posterior of the fixed effects in disease-mapping models. *Biometrics*, 62(4):1197–1206.
- [32] Reich, B. J., Yang, S., Guan, Y., Giffin, A. B., Miller, M. J., and Rappold, A. (2021). A review of spatial causal inference methods for environmental and epidemiological applications. *International Statistical Review*.
- [33] Rue, H. and Held, L. (2005). *Gaussian Markov Random Fields: Theory and Applications*. CRC press.
- [34] Ruppert, D., Wand, M. P., and Carroll, R. J. (2003). *Semiparametric regression*. Number 12. Cambridge university press.
- [35] Sarkar, D. (2008). *Lattice: Multivariate Data Visualization with R*. Springer, New York. ISBN 978-0-387-75968-5.
- [36] Schmidt, A. M. (2021). Discussion on “spatial+: A novel approach to spatial confounding” by emiko dupont, simon n. wood, and nicole h. augustin. *Biometrics*.

- [37] Thaden, H. and Kneib, T. (2018). Structural equation models for dealing with spatial confounding. *The American Statistician*, 72(3):239–252.
- [38] Waller, L. A. and Gotway, C. A. (2004). *Applied Spatial Statistics for Public Health Data*, volume 368. John Wiley & Sons.
- [39] Wickham, H. (2016). *ggplot2: Elegant Graphics for Data Analysis*. Springer-Verlag New York.
- [40] Wikle, C. K. (2010). Low-rank representations for spatial processes. In *Handbook of spatial statistics*, pages 114–125. CRC Press.
- [41] Yang, H.-D., Chiou, Y.-H., and Chen, C.-S. (2021). Estimation and selection for spatial confounding regression models. *Communications in Statistics-Theory and Methods*, pages 1–17.
- [42] Zimmerman, D. L. and Ver Hoef, J. M. (2021). On deconfounding spatial confounding in linear models. *The American Statistician*, pages 1–9.

## A Useful Facts about Differential Geometry and Linear Algebra

### A.1 Notation for metrics and norms

**Definition 1** (Standard Euclidean Inner Product and Norm). *We use the notation  $\langle \cdot, \cdot \rangle$  to denote the standard Euclidean inner product on the vector space of  $\mathbb{R}^n$ . The notation  $\|\cdot\|$  is then used to refer to the norm induced by this metric. Specifically, for  $\mathbf{a}, \mathbf{b} \in \mathbb{R}^n$ :*

$$\begin{aligned}\langle \mathbf{a}, \mathbf{b} \rangle &= \mathbf{a}^T \mathbf{b} \\ \|\mathbf{a}\| &= \sqrt{\mathbf{a}^T \mathbf{a}}\end{aligned}$$

**Notational Convention 1** (Angles with respect to the Standard Euclidean Inner Product). *Given  $\mathbf{a}, \mathbf{b} \in \mathbb{R}^n$ , we use  $\theta_{\mathbf{a}, \mathbf{b}}$  to refer to the angle between these two vectors with respect to the standard Euclidean norm. Specifically:*

$$\theta_{\mathbf{a}, \mathbf{b}} = \arccos \left( \frac{\langle \mathbf{a}, \mathbf{b} \rangle}{\|\mathbf{a}\| \|\mathbf{b}\|} \right)$$

**Notational Convention 2** (Spectral Decomposition of  $\hat{\Sigma}^{-1}$ ). *Let  $\hat{\Sigma}^{-1}$  be a  $n \times n$  real, symmetric, positive definite matrix.*

*We define  $\mathbf{U} \mathbf{D} \mathbf{U}^T = \hat{\Sigma}^{-1}$  to be the spectral decomposition of  $\hat{\Sigma}^{-1}$  with  $\mathbf{D}$  a diagonal matrix with diagonal  $d_1 \geq \dots \geq d_n > 0$ .*

**Notational Convention 3** (Angles between Vector and Eigenvectors of  $\hat{\Sigma}^{-1}$ ). *Let  $\hat{\Sigma}^{-1}$  be a  $n \times n$  real, symmetric, positive definite matrix, and  $\mathbf{v}$  be an arbitrary vector in  $\mathbb{R}^n$ .*

*Let  $\mathbf{U} \mathbf{D} \mathbf{U}^T = \hat{\Sigma}^{-1}$  be the spectral decomposition of  $\hat{\Sigma}^{-1}$  as defined in Notational Convention 2. In this paper, we use the notation  $\boldsymbol{\theta}_{\mathbf{v}, \mathbf{U}}$  to define a  $n \times 1$  vector whose  $i$ th element is the angle  $\theta_{\mathbf{v}, \mathbf{u}_i}$  (with respect to the Euclidean norm as in Notational Convention 1) between  $\mathbf{v}$  and the  $i$ th column  $\mathbf{u}_i$  of  $\mathbf{U}$ .*

**Definition 2** (Precision Matrix Induced Inner Product and Norm). *Given a  $n \times n$  real, symmetric, positive definite matrix,  $\hat{\Sigma}^{-1}$  we use the notation  $\langle \cdot, \cdot \rangle_{\hat{\Sigma}^{-1}}$  to denote the inner product defined by the matrix on the vector space of  $\mathbb{R}^n$ . The notation  $\|\cdot\|_{\hat{\Sigma}^{-1}}$  is then used to refer to the norm induced by this inner product. More precisely, for  $\mathbf{a}, \mathbf{b} \in \mathbb{R}^n$ :*

$$\begin{aligned}\langle \mathbf{a}, \mathbf{b} \rangle_{\hat{\Sigma}^{-1}} &= \mathbf{a}^T \hat{\Sigma}^{-1} \mathbf{b} \\ \|\mathbf{a}\|_{\hat{\Sigma}^{-1}} &= \sqrt{\mathbf{a}^T \hat{\Sigma}^{-1} \mathbf{a}}\end{aligned}$$

**Notational Convention 4** (Angles with respect to the Precision Matrix Induced Inner Product). *Given  $\mathbf{a}, \mathbf{b} \in \mathbb{R}^n$ , we use  $\phi_{\mathbf{a}, \mathbf{b}}$  to refer to the angle between them with respect to the standard Euclidean norm. Technically, it would be more appropriate to use  $\phi_{\mathbf{a}, \mathbf{b}}^{\hat{\Sigma}^{-1}}$ . However, we drop the dependency on  $\hat{\Sigma}^{-1}$  unless it is required for ease of reading. Specifically:*

$$\phi_{\mathbf{a}, \mathbf{b}} = \arccos \left( \frac{\langle \mathbf{a}, \mathbf{b} \rangle_{\hat{\Sigma}^{-1}}}{\|\mathbf{a}\|_{\hat{\Sigma}^{-1}} \|\mathbf{b}\|_{\hat{\Sigma}^{-1}}} \right)$$

## A.2 Useful Facts

**Fact 1** (Re-expression of Standard Euclidean Inner Product). *For  $\mathbf{a}, \mathbf{b} \in \mathbb{R}^n$ , the standard Euclidean metric defined in Definition 1 can be re-expressed as  $\langle \mathbf{a}, \mathbf{b} \rangle = \|\mathbf{a}\| \|\mathbf{b}\| \cos(\theta_{\mathbf{a}, \mathbf{b}})$ , where  $\theta_{\mathbf{a}, \mathbf{b}}$  is the angle between  $\mathbf{a}$  and  $\mathbf{b}$  with respect to the standard Euclidean metric as defined in Notational Convention 1.*

**Fact 2** (Re-expression of Precision Matrix Induced Inner Product). *For  $\mathbf{a}, \mathbf{b} \in \mathbb{R}^n$ , the precision matrix induced inner product defined in Definition 2 can be re-expressed as  $\langle \mathbf{a}, \mathbf{b} \rangle_{\hat{\Sigma}^{-1}} = \|\mathbf{a}\|_{\hat{\Sigma}^{-1}} \|\mathbf{b}\|_{\hat{\Sigma}^{-1}} \cos(\phi_{\mathbf{a}, \mathbf{b}})$ , where  $\phi_{\mathbf{a}, \mathbf{b}}$  is the angle between  $\mathbf{a}$  and  $\mathbf{b}$  with respect to the precision matrix induced metric as defined in Notational Convention 4.*

**Fact 3** (Preservation of Angles with Eigenvectors of  $\hat{\Sigma}^{-1}$ ). *Suppose  $\hat{\Sigma}^{-1}$  is a  $n \times n$  real, symmetric, positive definite matrix, and  $\mathbf{v}^s$  is an arbitrary unit vector with respect to the norm  $\|\cdot\|_{\hat{\Sigma}^{-1}}$  as defined in Definition 2 (i.e.,  $\|\mathbf{v}^s\|_{\hat{\Sigma}^{-1}} = 1$ ). Let  $\mathbf{v}_\alpha = \alpha \mathbf{v}^s$  for  $\alpha > 0$ . Define  $\theta_{\mathbf{v}^s, \mathbf{U}}$  and  $\theta_{\mathbf{v}_\alpha, \mathbf{U}}$  as in Notational Convention 3.*

*It is the case that  $\theta_{\mathbf{v}^s, \mathbf{U}} \equiv \theta_{\mathbf{v}_\alpha, \mathbf{U}}$ .*

**Fact 4** (Re-Expression of Precision Matrix Induced Norm). *For a given vector  $\mathbf{v} \in \mathbb{R}^n$  and  $n \times n$  real, symmetric, positive definite matrix  $\hat{\Sigma}^{-1}$ , it is possible to re-express  $\|\mathbf{v}\|_{\hat{\Sigma}^{-1}}$  as a function of the sample mean  $\bar{\mathbf{v}}$ , sample variance  $s_{\bar{\mathbf{v}}}^2$ , and a unique set of  $n$  angles (defined with respect to the standard Euclidean norm).*

*Let  $\mathbf{U} \mathbf{D} \mathbf{U} = \hat{\Sigma}^{-1}$  be the spectral decomposition of  $\hat{\Sigma}^{-1}$  with  $\mathbf{D}$  a diagonal matrix with diagonal  $d_1 \geq \dots \geq d_n > 0$ . Define  $\theta_{\mathbf{v}, \mathbf{U}}$  to be a  $n \times 1$  vector whose  $i$ th element is the angle  $\theta_{\mathbf{v}, \mathbf{u}_i}$  (with respect to the Euclidean norm as in Notational Convention 1) between  $\mathbf{v}$  and the  $i$ th column  $\mathbf{u}_i$  of  $\mathbf{U}$ .*

$$\|\mathbf{v}\|_{\hat{\Sigma}^{-1}} = \sqrt{[(n-1)s_{\bar{\mathbf{v}}}^2 + n\bar{\mathbf{v}}^2] \sum_{i=1}^n \cos^2(\theta_{\mathbf{v}, \mathbf{u}_i}) d_i}$$

**Fact 5** (Inner Products of Certain Kinds of Differences between Vectors). *Given an inner product  $\langle \cdot, \cdot \rangle_*$  on the vector space  $\mathbb{R}^n$  and a vector  $\mathbf{a} \in \mathbb{R}^n$ , let  $\mathbf{b} = [\mathbf{a} - \alpha \mathbf{1}]$  for  $\alpha \geq 0$ . Finally define  $\mathbf{c} \in \mathbb{R}^n$  to be an arbitrary vector. The following will hold*

1.  $\langle \mathbf{a}, \mathbf{b} \rangle_{\hat{\Sigma}^{-1}} = \|\mathbf{a}\|_{\hat{\Sigma}^{-1}}^2 - \alpha \langle \mathbf{a}, \mathbf{1} \rangle_{\hat{\Sigma}^{-1}}$
2.  $\langle \mathbf{b}, \mathbf{1} \rangle_{\hat{\Sigma}^{-1}} = \langle \mathbf{a}, \mathbf{1} \rangle_{\hat{\Sigma}^{-1}} - \alpha \|\mathbf{1}\|_{\hat{\Sigma}^{-1}}^2$
3.  $\|\mathbf{b}\|_{\hat{\Sigma}^{-1}}^2 = \|\mathbf{a}\|_{\hat{\Sigma}^{-1}}^2 - 2\alpha \langle \mathbf{a}, \mathbf{1} \rangle_{\hat{\Sigma}^{-1}} + \alpha^2 \|\mathbf{1}\|_{\hat{\Sigma}^{-1}}^2$
4.  $\langle \mathbf{b}, \mathbf{c} \rangle_{\hat{\Sigma}^{-1}} = \langle \mathbf{a}, \mathbf{c} \rangle_{\hat{\Sigma}^{-1}} - \alpha \langle \mathbf{c}, \mathbf{1} \rangle_{\hat{\Sigma}^{-1}}$

## B Proofs and Derivations

### B.1 Derivation of Remark 1 Non-Spatial Bias

$$\begin{aligned}
\mathbb{E}(\hat{\beta}_{NS} | \mathbf{X}^*) &= (\mathbf{X}^{*T} \mathbf{X}^*)^{-1} \mathbf{X}^{*T} (\beta_0 \mathbf{1} + \beta_x \mathbf{X} + \beta_z \mathbb{E}(\mathbf{Z} | \mathbf{X})) \\
&= \beta + \beta_z (\mathbf{X}^{*T} \mathbf{X}^*)^{-1} \mathbf{X}^{*T} \left( \mu_z \mathbf{1} + \rho \sigma_c \sigma_z \mathbf{C}(\theta_c)^T (\sigma_c^2 \mathbf{C}(\theta_c) + \sigma_u^2 \mathbf{C}(\theta_u))^{-1} \right. \\
&\quad \left. (\mathbf{X} - \mu_x \mathbf{1}) \right) \\
&= \beta + \beta_z (\mathbf{X}^{*T} \mathbf{X}^*)^{-1} \mathbf{X}^{*T} \left[ \mu_z \mathbf{1} + \rho \sigma_c \sigma_z (\sigma_c^2 \mathbf{I} + \sigma_u^2 \mathbf{C}(\theta_u) \mathbf{C}(\theta_c)^{-1})^{-1} \right. \\
&\quad \left. (\mathbf{X} - \mu_x \mathbf{1}) \right] \\
&= \beta + \beta_z \left[ \mu_z (\mathbf{X}^{*T} \mathbf{X}^*)^{-1} \mathbf{X}^{*T} \mathbf{1} + \rho \sigma_c \sigma_z (\mathbf{X}^{*T} \mathbf{X}^*)^{-1} \mathbf{X}^{*T} (\sigma_c^2 \mathbf{I} + \sigma_u^2 \mathbf{C}(\theta_u) \mathbf{C}(\theta_c)^{-1})^{-1} \right. \\
&\quad \left. (\mathbf{X} - \mu_x \mathbf{1}) \right] \\
&= \beta + \beta_z \left[ \mu_z \begin{bmatrix} 1 \\ 0 \end{bmatrix} + \rho \sigma_c \sigma_z (\mathbf{X}^{*T} \mathbf{X}^*)^{-1} \mathbf{X}^{*T} (\sigma_c^2 \mathbf{I} + \sigma_u^2 \mathbf{C}(\theta_u) \mathbf{C}(\theta_c)^{-1})^{-1} \right. \\
&\quad \left. (\mathbf{X} - \mu_x \mathbf{1}) \right] \\
&= \beta + \beta_z \left[ \mu_z \begin{bmatrix} 1 \\ 0 \end{bmatrix} + \rho \frac{\sigma_z}{\sigma_c} (\mathbf{X}^{*T} \mathbf{X}^*)^{-1} \mathbf{X}^{*T} \mathbf{K} (\mathbf{X} - \mu_x \mathbf{1}) \right]
\end{aligned}$$

where  $\mathbf{K} = p_c (p_c \mathbf{I} + (1 - p_c) \mathbf{C}(\theta_u) \mathbf{C}(\theta_c)^{-1})^{-1}$  and  $p_c = \frac{\sigma_c^2}{\sigma_c^2 + \sigma_u^2}$ . We now restrict our attention to the second element:

$$\mathbb{E}(\hat{\beta}_x^{NS} | \mathbf{X}^*) = \beta_x + \beta_z \rho \frac{\sigma_z}{\sigma_c} \left[ (\mathbf{X}^{*T} \mathbf{X}^*)^{-1} \mathbf{X}^{*T} \mathbf{K} (\mathbf{X} - \mu_x \mathbf{1}) \right]_2$$

## B.2 Derivation of Remark 1 Spatial Bias

$$\begin{aligned}
\mathbb{E}(\hat{\beta}^S | \mathbf{X}^*) &= \left( \mathbf{X}^{*T} \boldsymbol{\Sigma}^{-1} \mathbf{X}^* \right)^{-1} \mathbf{X}^{*T} \boldsymbol{\Sigma}^{-1} (\beta_0 \mathbf{1} + \beta_x \mathbf{X} + \beta_z \mathbb{E}(\mathbf{Z} | \mathbf{X})) \\
&= \beta + \left( \mathbf{X}^{*T} \boldsymbol{\Sigma}^{-1} \mathbf{X}^* \right)^{-1} \mathbf{X}^{*T} \boldsymbol{\Sigma}^{-1} \beta_z \left( \mu_z \mathbf{1} + \rho \sigma_c \sigma_z \mathbf{C}(\theta_c)^T (\sigma_c^2 \mathbf{C}(\theta_c) + \sigma_u^2 \mathbf{C}(\theta_u))^{-1} \right. \\
&\quad \left. (\mathbf{X} - \mu_x \mathbf{1}) \right) \\
&= \beta + \left( \mathbf{X}^{*T} \boldsymbol{\Sigma}^{-1} \mathbf{X}^* \right)^{-1} \mathbf{X}^{*T} \boldsymbol{\Sigma}^{-1} \beta_z \left[ \mu_z \mathbf{1} + \rho \sigma_c \sigma_z \left( \sigma_c^2 \mathbf{I} + \sigma_u^2 \mathbf{C}(\theta_u) \mathbf{C}(\theta_c)^{-1} \right)^{-1} \right. \\
&\quad \left. (\mathbf{X} - \mu_x \mathbf{1}) \right] \\
&= \beta + \beta_z \left[ \mu_z \begin{bmatrix} 1 \\ 0 \end{bmatrix} + \rho \sigma_c \sigma_z \left( \mathbf{X}^{*T} \boldsymbol{\Sigma}^{-1} \mathbf{X}^* \right)^{-1} \mathbf{X}^{*T} \boldsymbol{\Sigma}^{-1} \left( \sigma_c^2 \mathbf{I} + \sigma_u^2 \mathbf{C}(\theta_u) \mathbf{C}(\theta_c)^{-1} \right)^{-1} \right. \\
&\quad \left. (\mathbf{X} - \mu_x \mathbf{1}) \right] \\
&= \beta + \beta_z \left[ \mu_z \begin{bmatrix} 1 \\ 0 \end{bmatrix} + \rho \frac{\sigma_z}{\sigma_c} \left( \mathbf{X}^{*T} \boldsymbol{\Sigma}^{-1} \mathbf{X}^* \right)^{-1} \mathbf{X}^{*T} \boldsymbol{\Sigma}^{-1} \mathbf{K} (\mathbf{X} - \mu_x \mathbf{1}) \right]
\end{aligned}$$

where,  $\mathbf{K} = p_c \left( p_c \mathbf{I} + (1 - p_c) \mathbf{C}(\theta_u) \mathbf{C}(\theta_c)^{-1} \right)^{-1}$ ,  $p_c = \frac{\sigma_c^2}{\sigma_c^2 + \sigma_u^2}$ , and  $\boldsymbol{\Sigma} = \beta_z^2 \sigma_z^2 \mathbf{C}(\theta_c) + \sigma^2 \mathbf{I}$ . This calculation of the variance is done conditional on  $\mathbf{X}$  to mirror the results in Paciorek (26).

We restrict our attention to the second element, and note:

$$\mathbb{E}(\hat{\beta}_X^S | \mathbf{X}^*) = \beta_x + \beta_z \rho \frac{\sigma_z}{\sigma_c} \left[ \left( \mathbf{X}^{*T} \boldsymbol{\Sigma}^{-1} \mathbf{X}^* \right)^{-1} \mathbf{X}^{*T} \boldsymbol{\Sigma}^{-1} \mathbf{K} (\mathbf{X} - \mu_x \mathbf{1}) \right]_2$$

## B.3 Derivation of Lemma 1

$$\begin{aligned}
\mathbb{E}(\hat{\beta}^{NS}) &= \left( \mathbf{x}^{*T} \mathbf{x}^* \right)^{-1} \mathbf{x}^{*T} (\beta_0 \mathbf{1} + \beta_x \mathbf{x} + \beta_z \mathbf{z}) \\
&= \beta + \beta_z \left( \mathbf{x}^{*T} \mathbf{x}^* \right)^{-1} \mathbf{x}^{*T} \mathbf{z} \\
&= \beta + \beta_z \left( \begin{bmatrix} \mathbf{1}^T \mathbf{1} & \mathbf{1}^T \mathbf{x} \\ \mathbf{x}^T \mathbf{1} & \mathbf{x}^T \mathbf{x} \end{bmatrix} \right)^{-1} \mathbf{x}^{*T} \mathbf{z} \\
&= \beta + \frac{\beta_z}{\mathbf{1}^T \mathbf{1} \mathbf{x}^T \mathbf{x} - \mathbf{1}^T \mathbf{x} \mathbf{x}^T \mathbf{1}} \left( \begin{bmatrix} \mathbf{x}^T \mathbf{x} \mathbf{1}^T \mathbf{z} - \mathbf{1}^T \mathbf{x} \mathbf{x}^T \mathbf{z} \\ \mathbf{1}^T \mathbf{1} \mathbf{x}^T \mathbf{z} - \mathbf{x}^T \mathbf{1} \mathbf{1}^T \mathbf{z} \end{bmatrix} \right) \\
&= \beta + \frac{\beta_z}{\|\mathbf{1}\|^2 \|\mathbf{x}\|^2 - [\langle \mathbf{x}, \mathbf{1} \rangle]^2} \left[ \|\mathbf{x}\|^2 \langle \mathbf{z}, \mathbf{1} \rangle - \langle \mathbf{x}, \mathbf{1} \rangle \langle \mathbf{x}, \mathbf{z} \rangle \right. \\
&\quad \left. \left[ \|\mathbf{1}\|^2 \langle \mathbf{x}, \mathbf{z} \rangle - \langle \mathbf{x}, \mathbf{1} \rangle \langle \mathbf{z}, \mathbf{1} \rangle \right] \right].
\end{aligned}$$

Restricting our attention to the second element:

$$\mathbb{E} \left( \hat{\beta}_x^{NS} \right) = \beta_x + \frac{\beta_z}{\|\mathbf{1}\|^2 \|\mathbf{x}\|^2 - [\langle \mathbf{x}, \mathbf{1} \rangle \mathbf{x}^T]^2} (\|\mathbf{1}\|^2 \langle \mathbf{x}, \mathbf{z} \rangle - \langle \mathbf{x}, \mathbf{1} \rangle \langle \mathbf{z}, \mathbf{1} \rangle)$$

$$\text{Thus, Bias} \left( \hat{\beta}_x^{NS} \right) = \frac{\beta_z}{\|\mathbf{1}\|^2 \|\mathbf{x}\|^2 - [\langle \mathbf{x}, \mathbf{1} \rangle]^2} (\|\mathbf{1}\|^2 \langle \mathbf{x}, \mathbf{z} \rangle - \langle \mathbf{x}, \mathbf{1} \rangle \langle \mathbf{z}, \mathbf{1} \rangle)$$

## B.4 Proof of Lemma 2

$$\begin{aligned} \mathbb{E} \left( \hat{\beta}^g \right) &= \left( \mathbf{x}^{*T} \hat{\Sigma}^{-1} \mathbf{x}^* \right)^{-1} \mathbf{x}^{*T} \hat{\Sigma}^{-1} (\beta_0 \mathbf{1} + \beta_x \mathbf{x} + \beta_z \mathbf{z}) \\ &= \beta + \beta_z \left( \mathbf{x}^{*T} \hat{\Sigma}^{-1} \mathbf{x}^* \right)^{-1} \mathbf{x}^{*T} \hat{\Sigma}^{-1} \mathbf{z} \\ &= \beta + \beta_z \left( \begin{bmatrix} \mathbf{1}^T \hat{\Sigma}^{-1} \mathbf{1} & \mathbf{1}^T \hat{\Sigma}^{-1} \mathbf{x} \\ \mathbf{x}^T \hat{\Sigma}^{-1} \mathbf{1} & \mathbf{x}^T \hat{\Sigma}^{-1} \mathbf{x} \end{bmatrix} \right)^{-1} \mathbf{x}^{*T} \hat{\Sigma}^{-1} \mathbf{z} \\ &= \beta + \frac{\beta_z}{\mathbf{1}^T \hat{\Sigma}^{-1} \mathbf{1} \mathbf{x}^T \hat{\Sigma}^{-1} \mathbf{x} - \mathbf{1}^T \hat{\Sigma}^{-1} \mathbf{x} \mathbf{x}^T \hat{\Sigma}^{-1} \mathbf{1}} \left( \begin{bmatrix} \mathbf{x}^T \hat{\Sigma}^{-1} \mathbf{x} & -\mathbf{1}^T \hat{\Sigma}^{-1} \mathbf{x} \\ -\mathbf{x}^T \hat{\Sigma}^{-1} \mathbf{1} & \mathbf{1}^T \hat{\Sigma}^{-1} \mathbf{1} \end{bmatrix} \right) \mathbf{x}^{*T} \hat{\Sigma}^{-1} \mathbf{z} \\ &= \beta + \frac{\beta_z}{\mathbf{1}^T \hat{\Sigma}^{-1} \mathbf{1} \mathbf{x}^T \hat{\Sigma}^{-1} \mathbf{x} - \mathbf{1}^T \hat{\Sigma}^{-1} \mathbf{x} \mathbf{x}^T \hat{\Sigma}^{-1} \mathbf{1}} \begin{bmatrix} \mathbf{x}^T \hat{\Sigma}^{-1} \mathbf{x} & -\mathbf{1}^T \hat{\Sigma}^{-1} \mathbf{x} \\ -\mathbf{x}^T \hat{\Sigma}^{-1} \mathbf{1} & \mathbf{1}^T \hat{\Sigma}^{-1} \mathbf{1} \end{bmatrix} \begin{bmatrix} \mathbf{1}^T \hat{\Sigma}^{-1} \mathbf{z} \\ \mathbf{x}^T \hat{\Sigma}^{-1} \mathbf{z} \end{bmatrix} \\ &= \beta + \frac{\beta_z}{\mathbf{1}^T \hat{\Sigma}^{-1} \mathbf{1} \mathbf{x}^T \hat{\Sigma}^{-1} \mathbf{x} - \mathbf{1}^T \hat{\Sigma}^{-1} \mathbf{x} \mathbf{x}^T \hat{\Sigma}^{-1} \mathbf{1}} \begin{bmatrix} \mathbf{x}^T \hat{\Sigma}^{-1} \mathbf{x} \mathbf{1}^T \hat{\Sigma}^{-1} \mathbf{z} - \mathbf{1}^T \hat{\Sigma}^{-1} \mathbf{x} \mathbf{x}^T \hat{\Sigma}^{-1} \mathbf{z} \\ \mathbf{1}^T \hat{\Sigma}^{-1} \mathbf{1} \mathbf{x}^T \hat{\Sigma}^{-1} \mathbf{z} - \mathbf{x}^T \hat{\Sigma}^{-1} \mathbf{1} \mathbf{1}^T \hat{\Sigma}^{-1} \mathbf{z} \end{bmatrix} \\ &= \beta + \frac{\beta_z}{\|\mathbf{1}\|_{\hat{\Sigma}^{-1}}^2 \|\mathbf{x}\|_{\hat{\Sigma}^{-1}}^2 - [\langle \mathbf{x}, \mathbf{1} \rangle_{\hat{\Sigma}^{-1}}]^2} \left[ \frac{\|\mathbf{x}\|_{\hat{\Sigma}^{-1}}^2 \langle \mathbf{z}, \mathbf{1} \rangle_{\hat{\Sigma}^{-1}} - \langle \mathbf{x}, \mathbf{1} \rangle_{\hat{\Sigma}^{-1}} \langle \mathbf{x}, \mathbf{z} \rangle_{\hat{\Sigma}^{-1}}}{\|\mathbf{1}\|_{\hat{\Sigma}^{-1}}^2 \langle \mathbf{x}, \mathbf{z} \rangle_{\hat{\Sigma}^{-1}} - \langle \mathbf{x}, \mathbf{1} \rangle_{\hat{\Sigma}^{-1}} \langle \mathbf{z}, \mathbf{1} \rangle_{\hat{\Sigma}^{-1}}} \right]. \end{aligned}$$

Restricting our attention to the second element:

$$\mathbb{E} \left( \hat{\beta}_x^g \right) = \beta_x + \frac{\beta_z}{\|\mathbf{1}\|_{\hat{\Sigma}^{-1}}^2 \|\mathbf{x}\|_{\hat{\Sigma}^{-1}}^2 - [\langle \mathbf{x}, \mathbf{1} \rangle_{\hat{\Sigma}^{-1}}]^2} (\|\mathbf{1}\|_{\hat{\Sigma}^{-1}}^2 \langle \mathbf{x}, \mathbf{z} \rangle_{\hat{\Sigma}^{-1}} - \langle \mathbf{x}, \mathbf{1} \rangle_{\hat{\Sigma}^{-1}} \langle \mathbf{z}, \mathbf{1} \rangle_{\hat{\Sigma}^{-1}}).$$

## B.5 Derivation of Theorem 1

We assume that  $\mathbf{r}_x$  are the known residuals from a model of the form (3) with  $\mathbf{x}$  as the response and only an intercept. We assume that the model used to obtain these residuals gave an estimate of  $\hat{\Sigma}_x^{-1}$ . We note that this means

$$\mathbf{r}_x = \left[ \mathbf{I} - \mathbf{1} \left( \mathbf{1}^T \hat{\Sigma}_x^{-1} \mathbf{1} \right)^{-1} \mathbf{1}^T \hat{\Sigma}_x^{-1} \right] \mathbf{x}. \text{ For the following, we denote } \mathbf{r}_x^* = [\mathbf{1} \ \mathbf{r}_x].$$

$$\begin{aligned} \mathbb{E} \left( \hat{\beta}^h \right) &= \left( \mathbf{r}_x^{*T} \hat{\Sigma}^{-1} \mathbf{r}_x^* \right)^{-1} \mathbf{r}_x^{*T} \hat{\Sigma}^{-1} (\beta_0 \mathbf{1} + \beta_x \mathbf{x} + \beta_z \mathbf{z}) \\ &= \left( \mathbf{r}_x^{*T} \hat{\Sigma}^{-1} \mathbf{r}_x^* \right)^{-1} \mathbf{r}_x^{*T} \hat{\Sigma}^{-1} (\beta_0 \mathbf{1} + \beta_x \mathbf{x}) + \left( \mathbf{r}_x^{*T} \hat{\Sigma}^{-1} \mathbf{r}_x^* \right)^{-1} \mathbf{r}_x^{*T} \hat{\Sigma}^{-1} (\beta_z \mathbf{z}) \\ &= \mathbf{A}(\mathbf{r}_x, \mathbf{x}) + \mathbf{B}(\mathbf{r}_x, \mathbf{x}) \end{aligned} \tag{13}$$

The first term  $A(\mathbf{r}_x, \mathbf{x})$  is no longer simply  $\beta$  as it was in Appendix B.4. For clarity, we consider the two terms  $A(\mathbf{r}_x, \mathbf{x})$  and  $B(\mathbf{r}_x, \mathbf{x})$  separately.

**Simplifying  $A(\mathbf{r}_x, \mathbf{x})$**  In this sub-section, we focus on the first term of (13).

We employ the notation of Definition 2 in this section.

$$\begin{aligned}
A(\mathbf{r}_x, \mathbf{x}) &= \left( \mathbf{r}_x^{*T} \hat{\Sigma}^{-1} \mathbf{r}_x^* \right)^{-1} \mathbf{r}_x^{*T} \hat{\Sigma}^{-1} (\beta_0 \mathbf{1} + \beta_x \mathbf{x}) = \left[ \left( \begin{bmatrix} \mathbf{1}^T \hat{\Sigma}^{-1} \mathbf{1} & \mathbf{1}^T \hat{\Sigma}^{-1} \mathbf{r}_x \\ \mathbf{r}_x^T \hat{\Sigma}^{-1} \mathbf{1} & \mathbf{r}_x^T \hat{\Sigma}^{-1} \mathbf{r}_x \end{bmatrix} \right)^{-1} \mathbf{r}_x^{*T} \hat{\Sigma}^{-1} \mathbf{1} \beta_0 + \right. \\
&\quad \left. \left( \begin{bmatrix} \mathbf{1}^T \hat{\Sigma}^{-1} \mathbf{1} & \mathbf{1}^T \hat{\Sigma}^{-1} \mathbf{r}_x \\ \mathbf{r}_x^T \hat{\Sigma}^{-1} \mathbf{1} & \mathbf{r}_x^T \hat{\Sigma}^{-1} \mathbf{r}_x \end{bmatrix} \right)^{-1} \mathbf{r}_x^{*T} \hat{\Sigma}^{-1} \mathbf{x} \beta_x \right] \\
&= \frac{1}{\mathbf{1}^T \hat{\Sigma}^{-1} \mathbf{1} \mathbf{r}_x^T \hat{\Sigma}^{-1} \mathbf{r}_x - \mathbf{1}^T \hat{\Sigma}^{-1} \mathbf{r}_x \mathbf{r}_x^T \hat{\Sigma}^{-1} \mathbf{1}} \times \\
&\quad \left[ \begin{bmatrix} \mathbf{r}_x^T \hat{\Sigma}^{-1} \mathbf{r}_x \mathbf{1}^T \hat{\Sigma}^{-1} \mathbf{1} - \mathbf{1}^T \hat{\Sigma}^{-1} \mathbf{r}_x \mathbf{r}_x^T \hat{\Sigma}^{-1} \mathbf{1} \\ \mathbf{1}^T \hat{\Sigma}^{-1} \mathbf{1} \mathbf{r}_x^T \hat{\Sigma}^{-1} \mathbf{1} - \mathbf{r}_x^T \hat{\Sigma}^{-1} \mathbf{1} \mathbf{1}^T \hat{\Sigma}^{-1} \mathbf{1} \end{bmatrix} \beta_0 + \right. \\
&\quad \left. \begin{bmatrix} \mathbf{r}_x^T \hat{\Sigma}^{-1} \mathbf{r}_x \mathbf{1}^T \hat{\Sigma}^{-1} \mathbf{x} - \mathbf{1}^T \hat{\Sigma}^{-1} \mathbf{r}_x \mathbf{r}_x^T \hat{\Sigma}^{-1} \mathbf{x} \\ \mathbf{1}^T \hat{\Sigma}^{-1} \mathbf{1} \mathbf{r}_x^T \hat{\Sigma}^{-1} \mathbf{x} - \mathbf{r}_x^T \hat{\Sigma}^{-1} \mathbf{1} \mathbf{1}^T \hat{\Sigma}^{-1} \mathbf{x} \end{bmatrix} \beta_x \right] \\
&= \frac{1}{\|\mathbf{1}\|_{\hat{\Sigma}^{-1}}^2 \|\mathbf{r}_x\|_{\hat{\Sigma}^{-1}}^2 - [\langle \mathbf{r}_x, \mathbf{1} \rangle_{\hat{\Sigma}^{-1}}]^2} \times \\
&\quad \left[ \begin{bmatrix} \|\mathbf{1}\|_{\hat{\Sigma}^{-1}}^2 \|\mathbf{r}_x\|_{\hat{\Sigma}^{-1}}^2 - [\langle \mathbf{r}_x, \mathbf{1} \rangle_{\hat{\Sigma}^{-1}}]^2 \\ 0 \end{bmatrix} \beta_0 + \right. \\
&\quad \left. \begin{bmatrix} \|\mathbf{r}_x\|_{\hat{\Sigma}^{-1}}^2 \langle \mathbf{x}, \mathbf{1} \rangle_{\hat{\Sigma}^{-1}} - \langle \mathbf{r}_x, \mathbf{1} \rangle_{\hat{\Sigma}^{-1}} \langle \mathbf{r}_x, \mathbf{x} \rangle_{\hat{\Sigma}^{-1}} \\ \|\mathbf{1}\|_{\hat{\Sigma}^{-1}}^2 \langle \mathbf{r}_x, \mathbf{x} \rangle_{\hat{\Sigma}^{-1}} - \langle \mathbf{r}_x, \mathbf{1} \rangle_{\hat{\Sigma}^{-1}} \langle \mathbf{x}, \mathbf{1} \rangle_{\hat{\Sigma}^{-1}} \end{bmatrix} \beta_x \right]
\end{aligned}$$

Now, we restrict our attention to the second component. To further simplify we note that  $\mathbf{r}_x = [\mathbf{x} - \alpha \mathbf{1}]$  with  $\alpha = \frac{\langle \mathbf{x}, \mathbf{1} \rangle_{\hat{\Sigma}^{-1}}}{\|\mathbf{1}\|_{\hat{\Sigma}^{-1}}^2} \geq 0$ . We can therefore use



observations enumerated in Fact 5. to simply further:

$$\begin{aligned}
A_2(\mathbf{r}_x, \mathbf{x}) &= \frac{\beta_x \left( \|\mathbf{1}\|_{\hat{\Sigma}^{-1}}^2 \langle \mathbf{r}_x, \mathbf{x} \rangle_{\hat{\Sigma}^{-1}} - \langle \mathbf{r}_x, \mathbf{1} \rangle_{\hat{\Sigma}^{-1}} \langle \mathbf{x}, \mathbf{1} \rangle_{\hat{\Sigma}^{-1}} \right)}{\|\mathbf{1}\|_{\hat{\Sigma}^{-1}}^2 \|\mathbf{r}_x\|_{\hat{\Sigma}^{-1}}^2 - [\langle \mathbf{r}_x, \mathbf{1} \rangle_{\hat{\Sigma}^{-1}}]^2} \\
&= \frac{\beta_x \left( \|\mathbf{1}\|_{\hat{\Sigma}^{-1}}^2 \langle \mathbf{r}_x, \mathbf{x} \rangle_{\hat{\Sigma}^{-1}} - \langle \mathbf{r}_x, \mathbf{1} \rangle_{\hat{\Sigma}^{-1}} \langle \mathbf{x}, \mathbf{1} \rangle_{\hat{\Sigma}^{-1}} \right)}{\|\mathbf{1}\|_{\hat{\Sigma}^{-1}}^2 \|\mathbf{x}\|_{\hat{\Sigma}^{-1}}^2 - [\langle \mathbf{x}, \mathbf{1} \rangle_{\hat{\Sigma}^{-1}}]^2} \\
&= \text{Here we make use of the identities in Fact 5} \\
&= \frac{\beta_x \left( \|\mathbf{1}\|_{\hat{\Sigma}^{-1}}^2 \|\mathbf{x}\|_{\hat{\Sigma}^{-1}}^2 - [\langle \mathbf{x}, \mathbf{1} \rangle_{\hat{\Sigma}^{-1}}]^2 \right)}{\|\mathbf{1}\|_{\hat{\Sigma}^{-1}}^2 \|\mathbf{x}\|_{\hat{\Sigma}^{-1}}^2 - [\langle \mathbf{x}, \mathbf{1} \rangle_{\hat{\Sigma}^{-1}}]^2} \\
&= \beta_x
\end{aligned} \tag{14}$$

**Simplifying  $B(\mathbf{r}_x, \mathbf{x})$**  In this sub-section, we focus on the second term of (13). We again employ the notation of Definition 2. We note that the term is equivalent to the second term of Appendix B.4 with  $\mathbf{r}_x$  replacing  $\mathbf{x}$ . Therefore, we can borrow the result there to note:

$$\begin{aligned}
B(\mathbf{r}_x, \mathbf{x}) &= \left( \mathbf{r}_x^{*T} \hat{\Sigma}^{-1} \mathbf{r}_x^* \right)^{-1} \mathbf{r}_x^{*T} \hat{\Sigma}^{-1} (\beta_z \mathbf{z}) \\
&= \frac{\beta_z}{\|\mathbf{1}\|_{\hat{\Sigma}^{-1}}^2 \|\mathbf{r}_x\|_{\hat{\Sigma}^{-1}}^2 - [\langle \mathbf{r}_x, \mathbf{1} \rangle_{\hat{\Sigma}^{-1}}]^2} \left[ \|\mathbf{r}_x\|_{\hat{\Sigma}^{-1}}^2 \langle \mathbf{z}, \mathbf{1} \rangle_{\hat{\Sigma}^{-1}} - \langle \mathbf{r}_x, \mathbf{1} \rangle_{\hat{\Sigma}^{-1}} \langle \mathbf{r}_x, \mathbf{z} \rangle_{\hat{\Sigma}^{-1}} \right]
\end{aligned}$$

Note, that restricting our attention to the second component and again using Fact 5, we can further simplify as follows:

$$B_2(\mathbf{r}_x, \mathbf{x}) = \frac{\beta_z \left( \|\mathbf{1}\|_{\hat{\Sigma}^{-1}}^2 \langle \mathbf{r}_x, \mathbf{z} \rangle_{\hat{\Sigma}^{-1}} - \langle \mathbf{r}_x, \mathbf{1} \rangle_{\hat{\Sigma}^{-1}} \langle \mathbf{z}, \mathbf{1} \rangle_{\hat{\Sigma}^{-1}} \right)}{\|\mathbf{1}\|_{\hat{\Sigma}^{-1}}^2 \|\mathbf{r}_x\|_{\hat{\Sigma}^{-1}}^2 - [\langle \mathbf{r}_x, \mathbf{1} \rangle_{\hat{\Sigma}^{-1}}]^2}$$

Using the Fact 5 for the denominator

$$\begin{aligned}
&= \frac{\beta_z \left( \|\mathbf{1}\|_{\hat{\Sigma}^{-1}}^2 \langle \mathbf{r}_x, \mathbf{z} \rangle_{\hat{\Sigma}^{-1}} - \langle \mathbf{r}_x, \mathbf{1} \rangle_{\hat{\Sigma}^{-1}} \langle \mathbf{z}, \mathbf{1} \rangle_{\hat{\Sigma}^{-1}} \right)}{\|\mathbf{1}\|_{\hat{\Sigma}^{-1}}^2 \|\mathbf{x}\|_{\hat{\Sigma}^{-1}}^2 - [\langle \mathbf{x}, \mathbf{1} \rangle_{\hat{\Sigma}^{-1}}]^2} \\
&= \text{Using the Fact 5 for the numerator} \\
&= \frac{\beta_z \left( \|\mathbf{1}\|_{\hat{\Sigma}^{-1}}^2 \langle \mathbf{x}, \mathbf{z} \rangle_{\hat{\Sigma}^{-1}} - \langle \mathbf{x}, \mathbf{1} \rangle_{\hat{\Sigma}^{-1}} \langle \mathbf{z}, \mathbf{1} \rangle_{\hat{\Sigma}^{-1}} \right)}{\|\mathbf{1}\|_{\hat{\Sigma}^{-1}}^2 \|\mathbf{x}\|_{\hat{\Sigma}^{-1}}^2 - [\langle \mathbf{x}, \mathbf{1} \rangle_{\hat{\Sigma}^{-1}}]^2}
\end{aligned}$$

**Bias for  $\beta_x$**  Combining our results from (14) and (15):

$$\begin{aligned}
\mathbb{E} \left( \hat{\beta}^{AS} \right) - \beta_x &= A_2 \left( \mathbf{r}_x, \mathbf{x} \right) - \beta_x + B_2 \left( \mathbf{r}_x, \mathbf{x} \right) = \\
&\frac{\beta_z \left( \|\mathbf{1}\|_{\hat{\Sigma}^{-1}}^2 \langle \mathbf{x}, \mathbf{z} \rangle_{\hat{\Sigma}^{-1}} - \langle \mathbf{x}, \mathbf{1} \rangle_{\hat{\Sigma}^{-1}} \langle \mathbf{z}, \mathbf{1} \rangle_{\hat{\Sigma}^{-1}} \right)}{\|\mathbf{1}\|_{\hat{\Sigma}^{-1}}^2 \|\mathbf{x}\|_{\hat{\Sigma}^{-1}}^2 - \left[ \langle \mathbf{x}, \mathbf{1} \rangle_{\hat{\Sigma}^{-1}} \right]^2}
\end{aligned}$$